

Article

Catalytic CO₂ Activation Assisted by “Rhenium Hydride/B(C₆F₅)₃” Frustrated Lewis Pairs – Metal Hydrides Functioning as FLP Bases

Yanfeng Jiang, Olivier Blacque, Thomas Fox, and Heinz Berke

J. Am. Chem. Soc., **Just Accepted Manuscript** • DOI: 10.1021/ja402381d • Publication Date (Web): 25 Apr 2013

Downloaded from <http://pubs.acs.org> on May 6, 2013

Just Accepted

“Just Accepted” manuscripts have been peer-reviewed and accepted for publication. They are posted online prior to technical editing, formatting for publication and author proofing. The American Chemical Society provides “Just Accepted” as a free service to the research community to expedite the dissemination of scientific material as soon as possible after acceptance. “Just Accepted” manuscripts appear in full in PDF format accompanied by an HTML abstract. “Just Accepted” manuscripts have been fully peer reviewed, but should not be considered the official version of record. They are accessible to all readers and citable by the Digital Object Identifier (DOI®). “Just Accepted” is an optional service offered to authors. Therefore, the “Just Accepted” Web site may not include all articles that will be published in the journal. After a manuscript is technically edited and formatted, it will be removed from the “Just Accepted” Web site and published as an ASAP article. Note that technical editing may introduce minor changes to the manuscript text and/or graphics which could affect content, and all legal disclaimers and ethical guidelines that apply to the journal pertain. ACS cannot be held responsible for errors or consequences arising from the use of information contained in these “Just Accepted” manuscripts.



Catalytic CO₂ Activation Assisted by “Rhenium Hydride/B(C₆F₅)₃” Frustrated Lewis Pairs – Metal Hydrides Functioning as FLP Bases

Yanfeng Jiang, Olivier Blacque, Thomas Fox, Heinz Berke*

Anorganisch-chemisches Institut, Universität Zürich, Winterthurerstr. 190, CH-8037, Zürich, Switzerland.

Supporting Information Placeholder

ABSTRACT: Reaction of **1** with B(C₆F₅)₃ under 1 bar of CO₂ led to the instantaneous formation of the FLP type species [ReHBr(NO)(PR₃)₂(η²-O=C=O-B(C₆F₅)₃)] (**2**, R = *i*Pr **a**, Cy **b**) possessing two *cis*-phosphines and O_{CO₂} coordinated B(C₆F₅)₃ groups as verified by NMR spectroscopy and supported by DFT calculations. The attachment of B(C₆F₅)₃ in **2a,b** establishes cooperative CO₂ activation via the “Re-H/B(C₆F₅)₃” Lewis pair with the Re-H bond taking the role of a Lewis base. The Re(I) η¹-formato dimer [{Re(μ-Br)(NO)(η¹-OCH=O-B(C₆F₅)₃)(PPr₃)₂}] (**3a**) was generated from **2a** and represents the first example of a stable rhenium complex bearing two *cis*-aligned, sterically bulky PPr₃ ligands. Reaction of **3a** with H₂ cleaved the μ-Br bridges producing the stable and fully characterized formato dihydrogen complex [ReBrH₂(NO)(η¹-OCH=O-B(C₆F₅)₃)(PPr₃)₂] (**4a**) bearing *trans* phosphines. The stoichiometric CO₂ reduction of **4a** with Et₃SiH led to heterolytic splitting of H₂ along with formation of bis(triethylsilyl)acetal, (Et₃SiO)₂CH₂ (**7**). Catalytic reduction of CO₂ with Et₃SiH was also accomplished with the catalysts “**1a,b**/B(C₆F₅)₃”, **3a** and **4a** showing TOFs between 4 and 9 h⁻¹. The stoichiometric reaction of **4a** with the sterically hindered base TMP furnished H₂ ligand deprotonation. Hydrogenations of CO₂ using “**1a,b**/B(C₆F₅)₃”, **3a** and **4a** as catalysts gave in the presence of TMP TOFs of up to 7.5 h⁻¹ producing [TMPH][formate] (**11**). The influence of various bases (R₂NH, R = *i*Pr, Cy, SiMe₃; 2,4,6-tri-*tert*-butylpyridine, NEt₃, P^{*t*}Bu₃) was studied in greater detail pointing to two crucial factors of the CO₂ hydrogenations: the steric bulk and the basicity of the base.

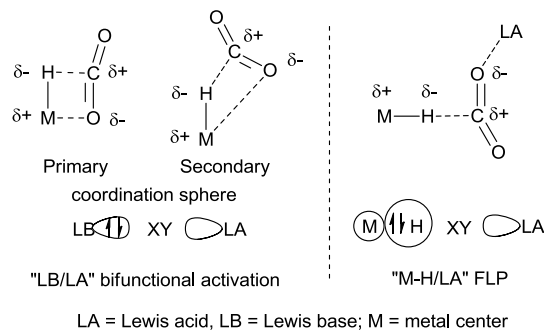
1. INTRODUCTION

CO₂ activation and reduction for alternative energy sources is a topic of current interest.¹ The major challenge originates from the high thermodynamic stability of CO₂, which calls for a remarkable driving force to ensure irreversible fixation. The currently developed chemical methods for CO₂ reduction could be classified into two categories based on either transition metals²⁻⁴ or main-group elements⁵⁻¹² using dihydrogen,² hydrosilanes³ and boranes⁴ as oxygen scavengers. One of the most prominent examples is the cooperative activation of CO₂ by frustrated Lewis pairs (FLPs), which consist of non- or weakly interacting Lewis acid and base pairs of the B/P,¹⁰ B/N,¹¹ or Al/P type.¹² FLPs are thus a milestone in the metal-free bifunctional activation of small molecules,^{8,9} but in addition they provide a non-classical way of activation using the polarizing power of electrostatic fields. In this context, the classical CO₂ insertion into a transition metal hydride bond could be viewed as a bifunctional activation or a FLP type activation process showing for the earlier process a vacant site at the metal center as the Lewis acid and for the latter process the hydride as the Lewis base. The FLP arrangement actually emphasizes the crucial role of the hydride component, which must be hydridic and consequently nucleophilic in character to enable interaction with the electrophilic carbon atom of CO₂.¹³

In line with the FLP notion we thus recognized that a transition metal hydride bond can be taken as “isolobal” to the free electron pair of a Lewis base, as depicted schematically in Scheme 1. The shape of the σ orbital of a M-H bond with sufficiently hydridic character resembles that of the lone pair electron of an organic Lewis base, which offers opportunity for activation by cooperation

with an external Lewis acid to form a “M-H/LA” FLP. In addition this structural arrangement would allow subsequent reactivity with hydride transfer as demonstrated by reports of Zr and Ru involved FLPs.¹⁴ Based on this idea, this paper demonstrates that rhenium hydride bonds can indeed act as a Lewis base in “Re-H/B(C₆F₅)₃” FLPs to activate and reduce CO₂.

Scheme 1. “Isolobal” analogy between a Lewis base and a metal hydride in the bifunctional or FLP activation process of CO₂ (or generally a XY molecule). Left: classical CO₂ bifunctional activation by M-H. Right: FLP type CO₂ activation by a M-H/LA system with the M-H unit as the Lewis base component.

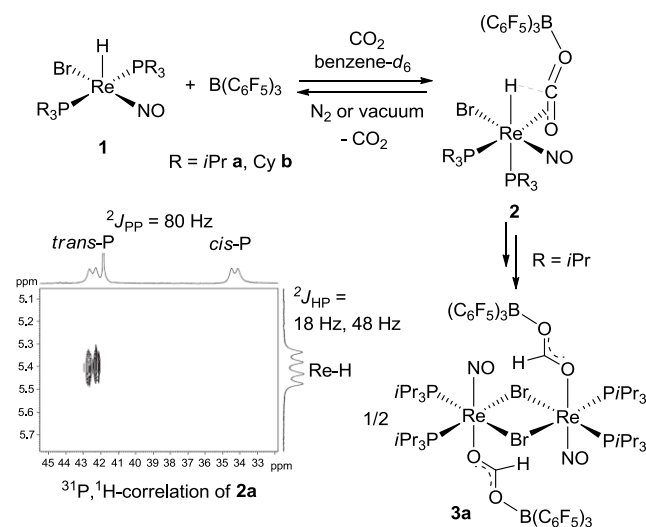


2. RESULTS AND DISCUSSIONS

2.1. Activation of CO₂ by the “Re-H/B(C₆F₅)₃” pair. The chemistry of the five-coordinate Re(I) hydride complexes [ReHBr(NO)-(PR₃)₂] (**1**, R = *i*Pr **a**, Cy **b**) was developed particularly with respect to catalysis.¹⁵ Due to its unsaturated 16e nature **1** shows strong affinities toward 2e donors, such as H₂, CO, O₂, ethylene, and carbenes.^{15b} However, no reaction was observed when for instance

the benzene-*d*₆ solution of **1a** or **1b** was exposed to 1 bar of CO₂ with spectroscopic monitoring. This reflected not only weak coordinating ability of CO₂, but maybe also insufficient hydridic and concomitant insufficient nucleophilic character of the Re-H bond for a secondary coordination sphere hydride transfer to CO₂. The position of the vacant site *trans* to the hydride also hampered the primary coordination sphere activation pathway. As verified additionally by ¹H, ³¹P and ¹⁹F NMR spectroscopy, no reaction occurred between the pairs “**1a,b** and B(C₆F₅)₃”, or “CO₂ and B(C₆F₅)₃”.

Scheme 2. CO₂ insertion into the Re-H bond of **1a,b** with B(C₆F₅)₃. The singlet observed in the ³¹P NMR spectrum was assigned to unreacted **1a**.



In contrast, when the **1a**/B(C₆F₅)₃ or **1b**/B(C₆F₅)₃ mixtures (1:1) were exposed to 1 bar of CO₂ in benzene-*d*₆, the original purple solutions immediately turned light brown affording within 20 min the six-coordinate 18e species **2** (R = *i*Pr **a**, Cy **b**) in 85 % *in-situ* yield, which were identified in solution as the Re(I) hydride structures of the type [ReHBr(NO)(PR₃)₂(*η*²-O=C=O-B(C₆F₅)₃)] possessing two *cis*-phosphines and a B(C₆F₅)₃-attached *η*²-CO₂ ligand (Scheme 2). The ¹H NMR spectrum revealed doublet resonances at 5.72 (**2a**) and 6.11 ppm (**2b**), which were assigned to the H_{Re} atoms. Surprisingly, two ²J_{PH} coupling constants of 18 and 48 Hz were observed, which indicated the presence of phosphine ligands *cis* and *trans* to the hydride. In the ³¹P NMR spectra, two doublets were observed at 39.6 and 33.0 ppm for **2a**, and at 30.0 and 22.1 ppm for **2b**, respectively. In comparison with the ²J_{PP} values of ca. 120 Hz observable for *trans*-bisphosphine ligands, the relatively small coupling constants of ca. 80 Hz in **2** further supported *cis*-alignment of the two phosphine ligands.¹⁵ The ¹H,³¹P-correlation spectrum of **2a** recorded at -60 °C revealed only correlation between the phosphorus signal at 39.6 ppm and that of the hydride indicative of their *trans* positions. The other phosphorus signal at 33.0 ppm showed no correlation to the hydride apparently suggesting their *cis* position. The ¹⁹F NMR spectra exhibited a new set of resonances at -134.97 (*o*-F), -160.07 (*p*-F), -166.55 (*m*-F) ppm for **2a**, and at -134.16 (*o*-F), -159.99 (*p*-F), -166.47 (*m*-F) ppm for **2b** providing evidence for the formation of the O-B(C₆F₅)₃ moiety.¹⁶ In the long range ¹³C, ¹H correlation spectrum of **2a** (HMBC) scalar couplings were observed between the hydride signal and the carbon resonances in the range of δ 150 to 135 ppm. This implied *η*² coordination of CO₂ *cis* to the Re-H bond, which enabled simultaneous interaction of the Re-H moiety

with the C_{OO2} atom and with the distantly coordinated B(C₆F₅)₃ moiety.

The CO₂ capture could be shown to be reversible, since exposure of the benzene solution of **2a,b** to N₂ or vacuum led to the quantitative regeneration of the free molecules **1a,b**, B(C₆F₅)₃ and CO₂, as evidenced for **1a,b** and B(C₆F₅)₃ by NMR spectroscopy. Addition of acetonitrile to the benzene solution of **2b** afforded instantaneously the CH₃CN-B(C₆F₅)₃ adduct concomitantly with the **1b**/CH₃CN adduct [ReHBr(NO)(PCy₃)₂(CH₃CN)]^{15b} possessing two *trans* phosphine ligands, further emphasizing the instability of **2a,b** envisaged to possess loosely bound CO₂.

The type **2** complexes appeared to be only intermittently stable even under 1 bar of CO₂ and gradually evolved into several new species within 4 h at 23 °C. The ¹H NMR spectrum then exhibited a new singlet at 9.61 ppm, which was correlated to a new singlet at 3.9 ppm in the ³¹P NMR spectrum. The ¹⁹F NMR spectrum revealed a new set of resonances at -133.62, -159.55 and -166.07 ppm. These were interpreted in terms of formation of a rhenium *η*¹-formate species with the terminal oxygen atom functionalized by B(C₆F₅)₃. This species was again seen to be transient, and gradually transformed into two other species revealing two singlets at 8.36 and 7.77 ppm in the ¹H NMR spectrum accompanied by two new singlets at 52.4 and 28.6 ppm in the ³¹P NMR and two new sets of signals at -134.18, -159.32, -166.06 ppm and at -133.68, -158.82, -165.07 ppm in the ¹⁹F NMR spectrum. Evidently, these data point to formation of two closely related rhenium formate isomers of as yet unknown detailed structures.

Interestingly, red-crystals gradually precipitated out from the benzene solution of **2a** along with the disappearance of **2a**. X-ray diffraction studies revealed a *μ*-Br bridged Re(I) dimer *η*¹-formate structure [Re(*μ*-Br)(NO)(*η*¹-OCH=O-B(C₆F₅)₃)(P*i*Pr₃)₂]₂ (**3a**) (Figure 1). Each center of the dimer adopts a pseudo-octahedral geometry. The B(C₆F₅)₃-coordinated formate moieties are located *trans* to the linear nitrosyl as a result of the strong *π*-donating/*π*-accepting push-pull effect. The most prominent structural feature is that the two phosphine ligands are *cis* showing a P-Re-P angle of 103.78(2)°. To the best of our knowledge, this is the first example of a *cis*-alignment of two sterically bulky P*i*Pr₃ ligands within the realm of rhenium complexes. Rare such cases of pseudo octahedral complexes with two *cis* P*i*Pr₃ ligands were observed previously in Os and Rh complexes.¹⁷ Noteworthy is the fact that in the solid state structure of **3a** the boron attached C-O bond (1.268(3) Å) is longer than that bonded to the Re center (1.246(2) Å), which is in accord with the conjugated character of the coordinated formate group characterized in solution.

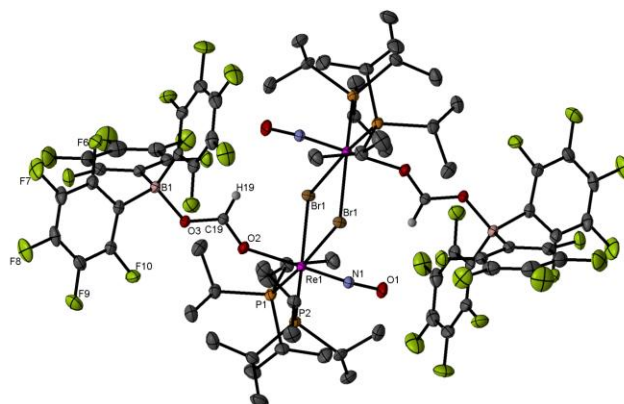


Figure 1. Molecular structure of **3a** with 30 % probability displacement ellipsoids. All hydrogen atoms were omitted for clarity except for the formate moieties. Selected bond lengths (Å) and angles (deg): N(1)-

O(1), 1.192(2); O(2)-Re(1), 2.1164(15); Re(1)-P(1), 2.4675(7); Re(1)-P(2), 2.4713(6); O(3)-B(1), 1.553(3); C(19)-O(2), 1.246(2); C(19)-O(3), 1.268(3); O(1)-N(1)-Re(1), 174.63(18); C(19)-O(2)-Re(1), 144.74(16); N(1)-Re(1)-O(2), 178.66(8); P(1)-Re(1)-P(2), 103.78(2); C(19)-O(3)-B(1), 126.52(18).

Similarly, **2b** slowly evolved under CO₂ atmosphere at 23 °C into three new rhenium formate species showing singlets at 9.57, 8.36 and 8.14 ppm in the ¹H NMR spectrum, which are correlated to three singlets at 25.1, 20.2 and 7.0 ppm in the ³¹P NMR spectrum. The species corresponding to the signal at 8.36 ppm remained as the major component after **2b** had completely disappeared within 15 h. In contrast to the case of **2a**, no precipitate was eventually formed. Particularly the ³¹P NMR spectrum of the solution indicated a complex mixture, from which attempts to isolate stable products proved to be unsuccessful. We however assume that the **2b** reactions proceeded along similar lines as that of **2a**.

Complex **3a** could be prepared in 72 % isolated yield from the reaction of **1a**/B(C₆F₅)₃ (1:1.5) with 1 bar of CO₂ in benzene after stirring at 23 °C for 24 h. In the IR spectrum, the expected $\nu(\text{NO})$ absorption is split revealing bands at 1708 and 1695 cm⁻¹. The $\nu(\text{OC}=\text{O})$ band was observed at 1592 cm⁻¹, which compared to

Lewis acid free [M-OCHO] species and is expected to have lowered $\nu(\text{OC}=\text{O})$ wavenumbers due to π -electron withdrawal induced by the B(C₆F₅)₃ attachment.¹⁸ For **3a** a satisfactory elemental analysis was obtained. NMR spectra of **3a** could not be recorded, due to insufficient solubility of this compound in non-coordinating solvents.

The structures of **2a,b** and related species along the CO₂ activation course were modelled by DFT calculations using PMe₃ model ligands. Based on the [ReHBr(NO)(PMe₃)₂] system with *trans* and *cis* PMe₃ ligands (denoted as “*transRe*” or “*cisRe*”), the reactions with CO₂ and BF₃ were explored. All optimized structures were found to be local energy minima. The model of **2a,b** (**V**) shows a pseudo-pentagonal bipyramidal geometry with a Br-Re-NO axis (Figure 2). CO₂ is η^2 -coordinated to the Re center and BF₃ weakly attached to the O_{CO2} atom showing a B-O distance of 1.633 Å. The relatively long Re-O distance of 2.243 Å speaks for a weakly bound CO₂ ligand, indeed consistent with the experimental observations for **2a,b**. The two PMe₃ ligands are disposed *cis* with a P-Re-P angle of 102.3°, which is quite comparable to that of the solid state structure of **3a**.

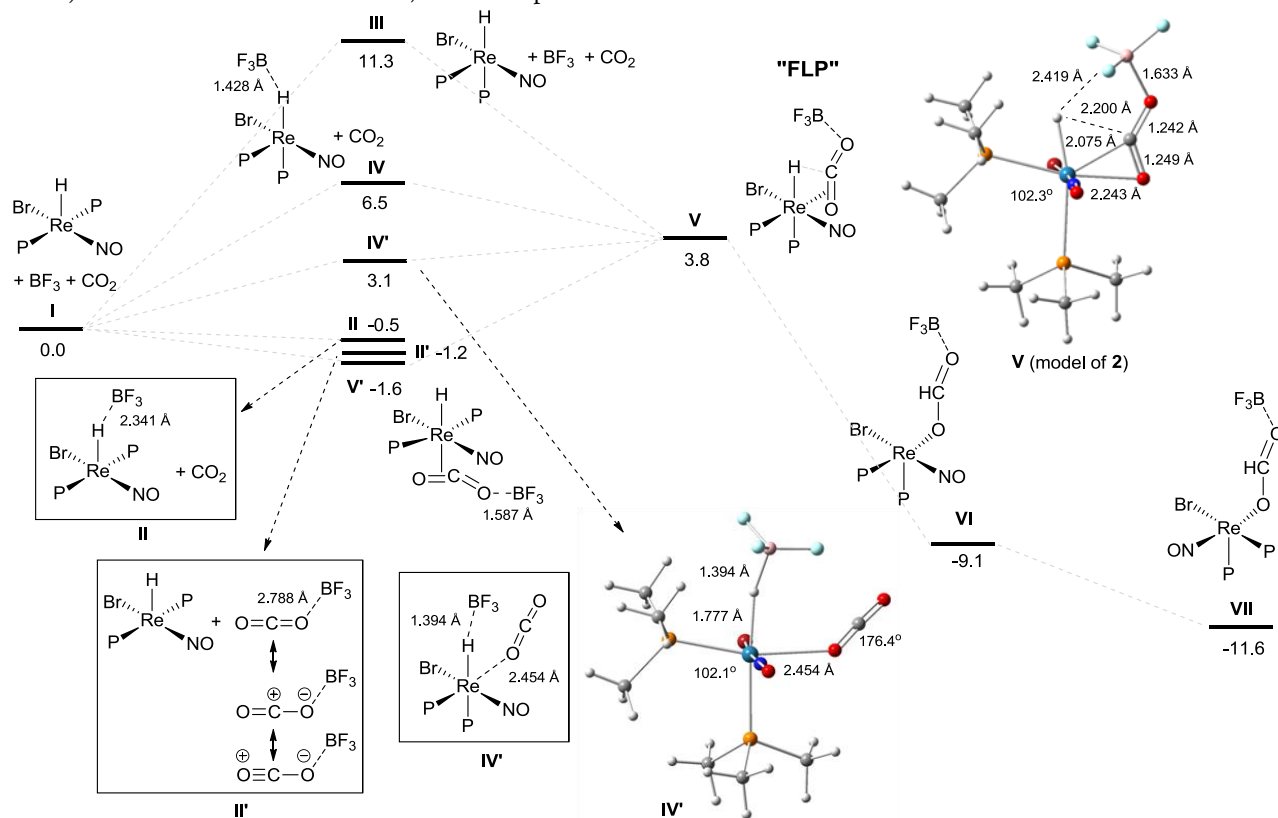


Figure 2. DFT calculated intermediates possibly involved in the CO₂ activation course with energies denoting local energy minima with respect to the reference (ΔE , kcal/mol)

The three free molecules of the *transRe*/CO₂/BF₃ arrangement **I** were taken as the energetic reference (0.0 kcal/mol). The energy of the mainly electrostatic binding of BF₃ to the Re-H bond in **II** was slightly endothermic (0.5 kcal/mol) showing a B-H bond distance of 2.341 Å. In the arrangement **II'** a B-O distance of 2.788 Å was observed suggesting weak electrostatic interactions with -1.2 kcal/mol of released energy. The BF₃-functionalized CO₂ can weakly coordinate to *transRe* showing in **V'** only -1.6 kcal/mol of stabilization energy. The two PMe₃ ligands are bent toward the hydride with a P-Re-P angle of 143.3°, which supposedly prevents

the insertion of the C=O bond into the *trans*-Re-H bond. On the other hand, the free *cisRe* molecule, CO₂ and BF₃ (**III**) are 11.3 kcal/mol higher in energy than the reference. The interaction between the BF₃ and the Re-H unit of *cisRe* is much stronger than that of **II** since a much shorter B-H distance of 1.428 Å was observed in **IV** showing an energy decrease of 4.8 kcal/mol relative to **III**. Coordination of CO₂ to the Re center of **IV** resulted in **IV'**, which lies 3.4 kcal/mol lower in energy than **IV**. The interaction between BF₃ and the Re-H unit in **IV'** became further enhanced showing a B-H distance of 1.394 Å. The CO₂ ligand remained

linear and was weakly bound to the Re center displaying a Re-O distance of 2.454 Å. Coordination of the BF₃-functionalized CO₂ to **cis**Re afforded **V**, which is 3.8 kcal/mol higher in energy than the reference, and -7.5 kcal/mol below **III**. Following the activation course of CO₂ by Re-H and BF₃ further afforded the model formato species **VI** releasing 12.9 kcal/mol in energy with respect to **V**. The isomerization of **VI** to **VII** bearing *trans*-aligned formato and nitrosyl ligands was found to be thermodynamically downhill by -2.5 kcal/mol. Furthermore, the dimerization via the bromo bridges led to a substantial thermodynamic stabilization of -15.5 kcal/mol.

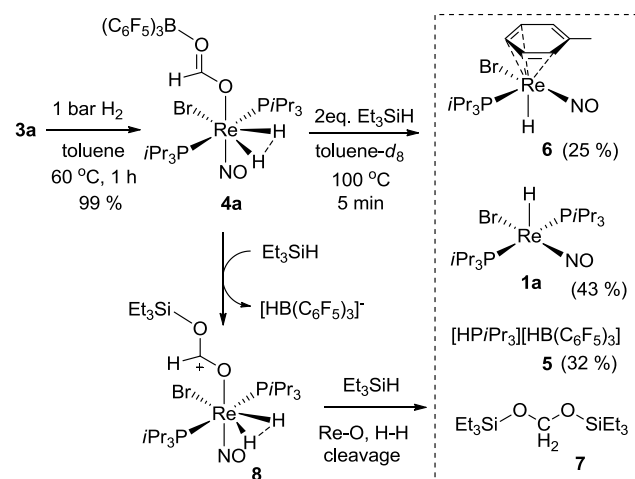
Based on these calculational results, we are inclined to propose that substitution of BF₃ by B(C₆F₅)₃ would additionally support the geometry change from the *trans*-phosphine to the *cis*-phosphine arrangements. Subsequently cooperative activation of CO₂ by the Re-H...B(C₆F₅)₃ FLP occurs in a similar fashion as for the Stephan type LB...B(C₆F₅)₃ FLPs by insertion of the substrate molecule in between the Lewis pair encounter complex. Such an activation course could initially be assisted by a η²-CO₂ π type interaction with the rhenium center, which similar as in **V** or **V'** helps to draw CO₂ closer to the Re-H and B(C₆F₅)₃ moieties.

2.2. Catalytic reduction of CO₂ with Et₃SiH. The μ-Br bridges can be cleaved by 2e donating molecules. For instance, under 1 bar of H₂ the suspension of **3a** in toluene afforded at 60 °C within 1 h the complex [ReBrH₂(NO)(η¹-OCH=OB(C₆F₅)₃)(P*i*Pr₃)₂] (**4a**) in 99 % isolated yield (Scheme 3). The IR spectrum revealed two characteristic intense bands: a ν(NO) band at 1741 cm⁻¹ and a ν(OC=O) band at 1595 cm⁻¹. The reaction with H₂ is assumed to lead to a “compressed dihydride” complex. The corresponding ¹H NMR resonance was observed as a relatively sharp triplet at 3.05 ppm, while the proton signal of the formato unit was found at 7.71 ppm in a typical region for H_{formato} substituents. The ³¹P NMR spectrum revealed a singlet resonance at 28.5 ppm suggesting two chemically equivalent *trans*-phosphine ligands. The presence of a O-B(C₆F₅)₃ moiety was indicated by the set of signals at -134.81, -157.74 and -164.98 ppm in the ¹⁹F NMR spectrum. As indicated by the ¹H NMR and by analogy to the reported dibromo dihydrogen Re(I) complexes,¹⁹ the H₂ ligand in **4a** is anticipated to also belong to the class of “compressed dihydrides” with a considerably elongated practically non-bonding H...H distance. This was supported further by DFT calculations on the model complex [ReBrH₂(η¹-OCH=OB(C₆F₅)₃)(NO)(P*i*Pr₃)₂], where the H...H distance turned out to be non-bonding at 1.50 Å.

Addition of 2 equiv. Et₃SiH to the light yellow toluene solution of **4a** afforded at 100 °C after 5 min a mixture in purple showing no trace of formato protons by ¹H NMR. Instead formation of the phosphonium borate [HP*i*Pr₃][HB(C₆F₅)₃] (**5**)²⁰ was observed exhibiting in the ¹H NMR spectrum a characteristic quartet of doublet signal at 4.40 ppm (¹J_{HP} = 453 Hz), which correlated with a singlet at 42.6 ppm in the ³¹P NMR spectrum formed in 32 % yield. The presence of the [HB(C₆F₅)₃]⁻ anion of **5** was confirmed by both a doublet signal at -19.45 ppm in the ¹¹B NMR and the set of resonances at -134.19, -164.48 and -167.95 ppm in the ¹⁹F NMR spectrum. Interestingly, a doublet signal at -7.61 ppm (²J_{HP} = 22 Hz) in the ¹H NMR spectrum could be spotted, which correlated with a phosphorus signal at 71.5 ppm in 25 % yield. This signal was assigned to a monophosphine hydride moiety [ReHBr(NO)(P*i*Pr₃)] presumably stabilized by an η⁴ toluene ligand (**6**)²¹ formed via heterolytic cleavage of the H-H bond in **4a** by dissociating a neighboring basic phosphine and deprotonation of the H₂ ligand.²² The ³¹P NMR spectrum also revealed the formation of **1a** in 43 % yield,

which definitely indicated that cleavage of the Re-O bond in **4a** by Et₃SiH had occurred.

Scheme 3. Formation of the “compressed dihydride” complex **4a** and its subsequent reaction with Et₃SiH



The ²⁹Si NMR spectrum revealed the presence of four silicon species showing singlets at 37.05, 30.01, 18.90 and 9.56 ppm. Among them the signal at 9.56 ppm was assigned to the [Et₃Si-H-B(C₆F₅)₃] adduct.²⁰ The resonance at 18.90 ppm represents the most prominent component, which corresponds to a singlet at 4.96 ppm in the ¹H NMR as revealed by the ¹H, ²⁹Si correlation spectrum. This evidently pointed to the formation of the bis(triethylsilyl)acetal (Et₃SiO)₂CH₂ (**7**), which was also observed by other CO₂ reduction systems using Et₃SiH as reducing agents, such as the “Zr/B(C₆F₅)₃” system reported by Matsuo and Kawaguchi,^{3b} the Iridium pincer catalyst by Brookhart et al.,^{3c} and the “TMP/B(C₆F₅)₃” system by Piers et al.^{11b} It is proposed that in a similar “tandem reaction” **4a** undergoes Et₃Si⁺ replacement of B(C₆F₅)₃ to form the [HB(C₆F₅)₃]⁻ and **8** (Scheme 3). The strong oxophilicity of the [Et₃Si]⁺ cation attached to the O_{CO2} atom weakens the Re-O bond in **8**, which then reacts further with Et₃SiH to afford **7** accompanied by H-H heterolytic cleavage yielding **5** and **6**.

In an attempt to accomplish catalytic reduction of CO₂ we used the “**1a**/B(C₆F₅)₃” system (1:1.5) and triethylsilane as a reductant under various conditions. In certain cases the silane functioned also as an oxygen scavenger (Table 1). Applying a catalyst loading of 1.0 mol% of **1a** and 1.5 mol% of B(C₆F₅)₃ in benzene-*d*₆ under 1 bar of CO₂ at 80 °C, 35 % of the Et₃SiH was converted to (Et₃SiO)₂CH₂ (**7**) within 4 h corresponding to a TON of 35 and a TOF of 8.8 h⁻¹. In this experiment no other silyl containing product could be observed by ¹H NMR spectroscopy.^{3b,3c,11b} GC-MS revealed the presence of small amounts of (Et₃Si)₂O, which however was anticipated to originate from the reaction of Et₃SiH with H₂O involved in the GC-MS manipulation. The “**1b**/B(C₆F₅)₃” system proved to be less efficient affording under the same conditions compound **7** in a TON of 18.

Significantly, the reaction catalyzed by 1 mol% of **4a** applying now 5 bar of CO₂ afforded at 80 °C within 13 h the silyl acetal **7** in 89 % yield, which corresponds to a TON of 89 and a TOF of 6.8 h⁻¹. A very small amount (3 %) of Et₃SiOCH₃ (**9**) was observed, which was recognized in the ¹H NMR spectrum as a singlet resonance at 3.32 ppm. We rationalized that **9** could be generated by the reaction of **7** with Et₃SiH. In addition the reaction produced (Et₃Si)₂O (**10**) in equivalent amounts to **9**.^{3b,3c,11b} The catalytic reduction of CO₂ using 1 mol% of **3a** and Et₃SiH produced **7** within 15 h in 87 %

yield corresponding to a TON of 87 and a TOF of 5.8 h⁻¹. Under the same conditions **3a** showed a slightly lower catalytic activity than **4a**, which was attributed to the lower solubility of **3a** in benzene. In the case of the catalysis with **3a**, product **9**, which requires an additional reduction step, was formed in only 1 % yield together with an equivalent (1 %) of **10**.

Table 1. Catalytic reduction of CO₂ by Et₃SiH

$$\text{Et}_3\text{SiH} + \text{CO}_2 \xrightarrow[\text{benzene, } 80^\circ\text{C}]{1.0 \text{ mol\% cat.}} (\text{Et}_3\text{SiO})_2\text{CH}_2 + \text{Et}_3\text{SiOMe} + (\text{Et}_3\text{Si})_2\text{O}$$

Entry	cat.	P _{CO₂} (bar)	t(h)	Yield (%) ^a 7 / 9 / 10	TON	TOF (h ⁻¹)
1	1a /B(C ₆ F ₅) ₃ ^b	1	4	35 / 0 / 0	35	8.8
2	1b /B(C ₆ F ₅) ₃ ^b	1	4	18 / 0 / 0	18	4.5
3	3a	5	15	87 / 1 / 1	89	5.9
4	4a	5	13	89 / 3 / 3	95	7.3

^a Determined by GC-MS. ^b In a ratio of 1:1.5

2.3. Catalytic CO₂ hydrogenation in the presence of base. Catalytic hydrogenation of CO₂ was carried out with the “**1**/B(C₆F₅)₃” system, but additionally in presence of the sterically hindered Lewis base TMP (2,2,6,6-tetramethylpiperidine). Under 20 bar of CO₂ and 40 bar of H₂ in THF with 1 mmol of TMP, the “**1a**/B(C₆F₅)₃” system (0.5 mol%, 1:2) afforded at 80 °C within 15 h the piperidinium formate salt [H-TMP]⁺[O-CH=O]⁻ (**11**) in 52 % yield corresponding to a TON of 104 (entry 2, Table 2). Formation of the related formamide could not be observed.²³ The same reaction afforded within 2 h a TON of 16 indicating a slow turnover rate (entry 3, Table 2). A blank reaction in the absence of “**1**/B(C₆F₅)₃” did not afford hydrogenation at all (entry 4, Table 2). THF turns out to be an appropriate solvent for these catalyses, most probably due to its efficient solvation effect. The reaction in chlorobenzene or methanol showed under the same condition lower activities (entries 1 and 12, Table 2). At 23 °C hydrogenation of CO₂ did not take place (entry 5, Table 2). Increasing the temperature to 120 °C resulted also in a poor TON (entry 6, Table 2), which was attributed to increased decomposition of the active species. Decreasing the H₂ and CO₂ pressures to 20 and 10 bar resulted in a very small TOF (entry 7, Table 2), which was interpreted in terms of the inability to accumulate sufficient kinetically relevant concentrations of **4a**.

Remarkably, when **4a** was used as a catalyst in the absence of additional B(C₆F₅)₃, the hydrogenation of CO₂ in THF with 1 mmol of TMP at 80 °C afforded within 15 h a TON value of 92 (entry 10, Table 2), which is quite comparable to that of the “**1a**/B(C₆F₅)₃” experiment. This indicated that complexes of type **4a** might be involved as intermediates in the various reaction courses. In comparison to **4a**, the activity of **3a** was found to be slightly lower giving under the same conditions a TON of 72, presumably caused by the low solubility of **3a** in THF (entry 9, Table 2).

Table 2. Catalytic hydrogenation of CO₂ in the presence of TMP

$$\text{CO}_2 + \text{H}_2 + \text{1 mmol} \xrightarrow[\text{(0.5 mol\%)}]{[\text{Re}]/\text{B}(\text{C}_6\text{F}_5)_3 \text{ (1:2)}} \text{H-C(=O)-O}^- \text{H}_2\text{N}^+ \text{11}$$

Entry	[Re]	solvent	T(°C)	P _{H₂/CO₂} (bar)	t(h)	Conv. (%) ^a	TON	TOF (h ⁻¹)
1	1a	C ₆ H ₅ Cl	80	40/20	15	8	15	1.0
2	1a	THF	80	40/20	15	52 ^b	104	6.9
3	1a	THF	80	40/20	2	8	16	7.5
4	--	THF	80	40/20	24	0	0	0
5	1a	THF	23	40/20	18	0	0	0
6	1a	THF	120	40/20	18	3	6	0.3
7	1a	THF	80	20/10	15	4	8	0.4
8	1b	THF	80	40/20	16	28	55	3.4
9 ^c	3a	THF	80	40/20	15	36	72	4.8
10 ^c	4a	THF	80	40/20	15	46	92	6.1
11 ^c	1a	THF	80	40/20	15	39	78	5.2
12 ^c	1a	MeOH	80	40/20	15	25	50	3.3

^a Determined by referring to the internal standard DMF in ¹H NMR spectra. ^b in 20 % isolated yield. ^c in the absence of B(C₆F₅)₃

The molecular structure of **11** was established by both NMR spectroscopy and an X-ray diffraction study, as depicted in Figure 3. Moderately strong intermolecular hydrogen bonding was observed between the NH proton and the formate oxygen atom.²⁴

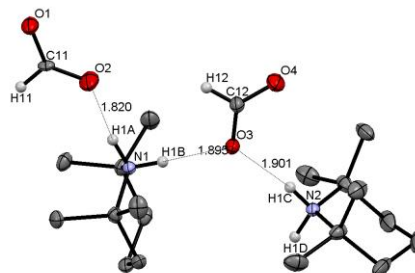


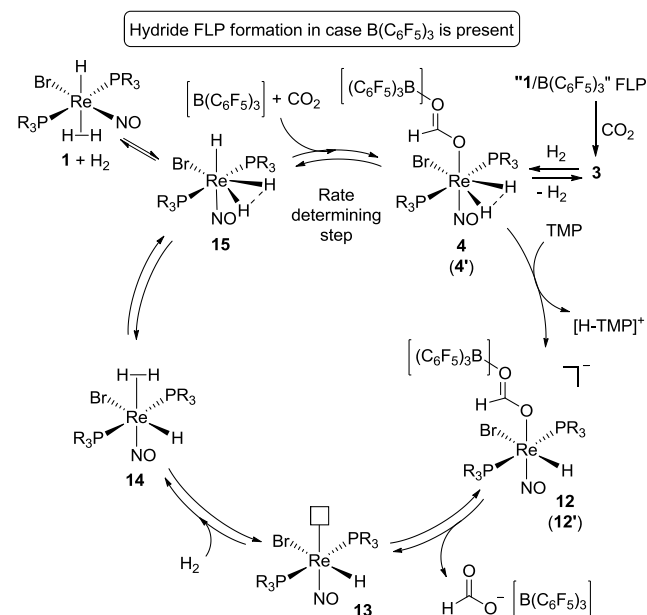
Figure 3. Molecular structure of **11** with 30 % probability displacement ellipsoids. All hydrogen atoms were omitted for clarity except for the formate and NH₂ moieties.

To obtain further insight into the reaction mechanism, stoichiometric reactions of the catalyst were investigated. When **4a** was mixed with 2 equiv. of TMP at 23 °C in THF-*d*₆, the solution instantaneously turned purple with a white precipitate formed. In the ¹H NMR spectrum a triplet resonance at -6.53 ppm (*J*_{HP} = 15 Hz) and a broad singlet at -15.22 ppm were observed, which correlated with two singlets at 41.8 and 40.8 ppm in the ³¹P NMR spectrum. The triplet signal was assigned to a *trans* diphosphine Re-H species generated via deprotonation of the H₂ moiety. The broad singlet at -15.22 ppm was characteristic for the hydride **1a**.^{15a} Both observations implied TMP assisted heterolytic cleavage followed by dissociation of the formate ligand from the Re center of **4a**. The white precipitate could be ascertained to be the piperidinium formate **11**, which was partly still present in solution as confirmed by ¹H NMR spectroscopy. Products relating back to reactions with the “TMP/B(C₆F₅)₃” FLP and CO₂ or H₂ could not be detected.^{11,8}

The above results pointed to a CO₂ hydrogenation mechanism in presence of B(C₆F₅)₃, as proposed in Scheme 4. Like in a FLP the activation pathway starts with the interaction of the hydride ligand of the “**1**/B(C₆F₅)₃” pair with CO₂ to give **3**, which further reacts with H₂ to afford the formate dihydrogen complexes of type **4**. It should be noted at this point that the cycle is assumed to be driven

by complexes with *trans* phosphine arrangements. The *cis* phosphine complexes of type **3** are assumed to function as resting states outside the catalytic cycle. In the presence of the sterically hindered Lewis base TMP, deprotonation of the H₂ ligand occurs affording the [HTMP]⁺ cation and the anionic Re-H formate complex **12** in full agreement with the observations of the described stoichiometric reaction.²² **12** is prepared for formate elimination and exchange with H₂ via a 16e rhenium hydride species **13** to form **14**, since the π donor formate feels strong repulsion from the filled d orbitals of the rhenium center. The repulsion is even enhanced by the fact that the complex is anionic and loaded with charge. Subsequently the *trans* dihydrogen hydride complex **14** is anticipated to rearrange to the isomeric “compressed dihydride hydride **15** via a trihydride transition state.²⁵ Related rhenium complexes showed in H₂/D₂ scrambling experiments similar dihydrogen hydride exchange courses.^{15e} DFT calculations using the [ReHBr(NO)(PMe₃)₂] model fragment suggest a practically thermoneutral process for the conversion of **13** to **14** revealing the minute energy difference of -0.1 kcal/mol between the model complexes of **13**/H₂ and **14**. Similarly the isomerization step from **14** to **15** can be anticipated to be mildly “exothermic”, since the calculations of the corresponding model complexes brought about a -6.0 kcal/mol energy difference.

Scheme 4. Sketch of a catalytic cycle for CO₂ hydrogenation in presence of TMP displaying the type **1**, **3** and **4** compounds in presence and absence of B(C₆F₅)₃. Those species appearing in absence of B(C₆F₅)₃ are denoted as **4'** and **12'**.



It should be noted at this point that H₂ ligands *trans* to a strong donor, like the hydride ligand and *trans* to a strong π acceptor are expected to possess a H₂ ligand structure, while H₂ ligands *trans* to a π donor like halogen ligands should reveal an elongated dihydrogen or compressed dihydride structure.²⁶ In the catalytic reaction course **1** could possess higher concentrations similar to a resting state, since it precedes the rate determining step.^{15b} According to Scheme 4 **15** and B(C₆F₅)₃ constitute the catalytically crucial “Re-H/B(C₆F₅)₃” FLP, which activates CO₂ and regenerates the type **4** complexes. The deprotonation step of **4**(**4'**) could principally be slow and rate determining, since the “compressed dihydrides” of type **4** are expected to be less acidic than dihydrogen complexes. Nevertheless, the stoichiometric deprotonation of **4a** proceeded instantaneously at ambient temperature, which indicates that the

given “compressed dihydrides” are more acidic. Therefore the regeneration step of **4**(**4'**) preceding the deprotonation is presumed to be rate determining. In the earlier context the stoichiometric reaction sequence of **1a**/B(C₆F₅)₃ with CO₂ and subsequently with H₂ has been shown to be overall very slow at room temperature. The related transformation, which constitutes insertion of CO₂ into the Re-H bond, is expected to be slow even at the higher temperature of 80 °C of the catalyses. Therefore we rationalized that this step would be the slowest of all steps of the catalytic cycle and rate determining.

It should also be noted that the 1/B(C₆F₅)₃/CO₂/H₂ reaction mixture contains not only the 1/B(C₆F₅)₃ FLP, but also the “classical” metal-free TMP/B(C₆F₅)₃ FLP. Competitive FLP reactivity can be envisaged to occur with simultaneous capture of CO₂ and H₂ by this FLP leading to the formation of a [H-TMP][O=CH-OB(C₆F₅)₃] product or by H₂ embracement to the [H-TMP][HB(C₆F₅)₃] salt.^{11, 8} In the presence of **1a** however both these FLP reaction channels seemed not to be competitive with the reactions of the 1/B(C₆F₅)₃ FLP, as implied by entry 4 in Table 2.

Table 3. Comparison of the performance of different bases in catalytic hydrogenation of CO₂

		0.5 mol% [Re] 1.0 mol% B(C ₆ F ₅) ₃					
CO ₂ + H ₂ + base		THF, 80 °C		H-C(=O)-O ⁻ [H-base] ⁺			
20 bar 40 bar 1 mmol							
Entry	[Re]	base	product	t(h)	Conv. (%) ^a	TON	TOF (h ⁻¹)
1	1a			34	87 ^b	174	5.1
2	1b			36	67	134	3.7
3 ^c	1a			15	27	54	3.6
4	1a			22	3	7	0.3
5	1b	NEt ₃		28	5	10	0.4
6 ^c	1a			18	3	6	0.3
7	1a	PfBu ₃	---	16	<1	--	--
8	1a			30	61 ^d	122	4.1
9 ^c	1a			20	34	68	3.4
10	1a	HN(SiMe ₃) ₂		16	2	4	0.2
11 ^e	1a		---	6	--	--	--

^a Determined by referring to the internal standard DMF in ¹H NMR spectra. ^b in 12 % isolated yield. ^c in the absence of B(C₆F₅)₃. ^d In 13 % isolated yield. ^e with 10 mol% of **1a**/B(C₆F₅)₃ (1:2)

The potential of the catalytic CO₂ hydrogenation applying **1a** was additionally explored in the absence of B(C₆F₅)₃, which surprisingly afforded under the same conditions as in the presence of B(C₆F₅)₃ a TON of 78 (entry 11, Table 2). Thus, **1a** alone appeared to be a good, but somewhat less active catalyst than the cocatalytic system **1a**/B(C₆F₅)₃. We assume that this catalysis follows a similar reaction course with formation of the B(C₆F₅)₃ free formate rhenium species **4'**. The secondary coordination sphere hydride transfer from **15** onto CO₂ does not contrast the observation that **1** does not react with CO₂, since the reactive species **14** are isomeric to **1**. Structures of type **14** are expected to possess a

more hydridic character in the Re-H bonds than **1**, which originates from the *trans* influence of the *trans* positioned NO ligand. The H₂ ligand of **4'** is however expected to be less acidic than that of **4**, since the B(C₆F₅)₃ substituent of **4** leads to additional electron withdrawal affecting also the H₂ ligand.

In a tuning effort different bases of various base strengths were then tested for the performance in the hydrogenation of CO₂. Exclusive formation of the corresponding formate salts was invariably observed instead of the alternative formation of formamide compounds (Table 3). In the case of the sterically less demanding base HN*i*Pr₂, the catalytic system of "**1a**/B(C₆F₅)₃" afforded the formate salt [HN*i*Pr₂]⁺[O-CH=O]⁻ (**16**) within 34 h in 87 % yield corresponding to a TON of 174 and a TOF of 5.1 h⁻¹ (entry 1, Table 3). The "**1b**/B(C₆F₅)₃" system was found here to be slightly less active. Within 36 h a TON of 134 was accomplished (entry 2, Table 3). The reaction with the least bulky amine NEt₃ afforded under the same conditions poorer TONs of up to 10 within 28 h (entries 4 and 5, Table 3). By comparison, HNCy₂ as a base furnished a conversion of 61 % and a TON of 122 using the "**1a**/B(C₆F₅)₃" co-catalytic system with formation of the [HN-Cy₂]⁺[O-CH=O]⁻ (**17**) salt (entry 8, Table 3). These results evidently pointed out that steric hindrance of the employed base is key to the efficiency of the CO₂ hydrogenation. Another crucial factor is apparently the basicity of the base. In the case of P*t*Bu₃, which is sterically bulky, but much less basic than the secondary amines, nearly no catalytic activity was observed (entry 7, Table 3). The NMR spectrum revealed a complex mixture possibly containing the CO₂ captured product [P*t*Bu₃-P-C(=O)-O-B(C₆F₅)₃] originating from the reaction of CO₂ with the "P*t*Bu₃/B(C₆F₅)₃" FLP.^{10a} However, the H₂ activated product [HP*t*Bu₃][HB(C₆F₅)₃] was not observed. The crucial role of the basicity of the base was further supported by the reaction using HN(SiMe₃)₂, which is bulkier, but less basic than HN*i*Pr₂. Indeed, a very poor TON of 4 was obtained within 16 h under the same catalytic conditions as for the other base reactions (entry 10, Table 3). 2,4,6-tri-*tert*-butylpyridine also showed no conversion in the CO₂ hydrogenation attributed to its too low basicity (entry 11, Table 3). Finally it should be mentioned that in all cases of secondary amines the CO₂ hydrogenations catalyzed by **1a** were also examined in the absence of B(C₆F₅)₃. Invariably inferior catalytic performances compared to those in the presence of B(C₆F₅)₃ were observed.

3. CONCLUSIONS

In conclusion, we demonstrated that cooperative FLP type activation of CO₂ can be accomplished by "Re-H/B(C₆F₅)₃" systems with the Re-H bond operating as the Lewis base component. These FLPs rendered subsequent catalytic reduction of CO₂ by a hydrosilane, and catalytic hydrogenation of CO₂ in the presence of sterically hindered strong bases. This work therefore not only emphasized the possibility for extending the scope of the FLP concept into transition metal hydrides as bases components to get involved in small molecules activations, but also demonstrated that FLP tuning of non-platinum-group transition metals may provide ample opportunity for catalytic CO₂ reduction. Explorations of related but more efficient catalytic CO₂ hydrogenation processes are currently underway in our group.

EXPERIMENTAL SECTION

General Experimental. All manipulations were carried out under an atmosphere of dry nitrogen using standard Schlenk techniques or in a glovebox (M. Braun 150B-G-II) filled with dry nitrogen. Solvents were freshly distilled under N₂ by employing standard procedures and were

degassed by freeze-thaw cycles prior to use. The deuterated solvent CD₂Cl₂ was dried over molecular sieves, benzene-*d*₆ and toluene-*d*₈ were dried with sodium/benzophenone and vacuum transferred for storage in a Schlenk flask fitted with Teflon valves. ¹H NMR, ¹³C{¹H}-NMR, ³¹P{¹H}-NMR, ¹⁹F NMR and ¹¹B NMR data were recorded on a Varian Mercury 300 spectrometer using 5 mm diameter NMR tubes equipped with Teflon valves, which allow degassing and further introduction of gases into the probe. Chemical shifts are expressed in parts per million (ppm). ¹H and ¹³C{¹H}-NMR spectra were referenced to the residual proton or ¹³C resonances of the deuterated solvent. All chemical shifts for the ³¹P{¹H}-NMR data are reported downfield in ppm relative to external 85 % H₃PO₄ at 0.0 ppm. Signal patterns are reported as follows: s, singlet; d, doublet; t, triplet; m, multiplet. IR spectra were obtained by using ATR methods with a Bio-Rad FTS-45 FTIR spectrometer. Complexes **1** were prepared according to reported procedures.^{15a}

[{Re(μ-Br)(NO)(*η*¹-OCH=OB(C₆F₅)₃)(P*i*Pr₃)₂}]₂ (3a**):** In a 30 mL Young-tap Schlenk vessel, 62.0 mg [ReHBr(NO)(P*i*Pr₃)₂] (**1a**, 0.10 mmol) was mixed in a glove-box with 71.5 mg B(C₆F₅)₃ (0.14 mmol) in 5 mL benzene. The N₂ atmosphere was replaced with 1.0 bar of CO₂ using the freeze-pump-thaw cycle. After warming to room temperature, the originally violet solution instantaneously turned brown. The mixture was kept stirring at room temperature for overnight leading to the formation of a large amount of a pale-red precipitate, which was isolated and further washed with benzene (1 x 1 mL) and pentane (3 x 3 mL), dried *in vacuo* affording a pale-red solid: 84.0 mg. Yield: 72 %. IR (cm⁻¹, ATR): ν (NO) 1708, 1695; ν (OC=O) 1592. Anal. Calcd for C₇₄H₈₆B₂Br₂F₃₀N₂O₆P₄Re₂ (2347.18): C, 37.87; H, 3.69; N, 1.19. Found: C, 37.48; H, 3.85; N, 1.09.

Reaction of **1a with B(C₆F₅)₃ and CO₂ in the NMR tube.** In a 3 mL Young-tap NMR-tube, 12.4 mg **1a** (0.02 mmol) was mixed with 30.2 mg B(C₆F₅)₃ (0.06 mmol, 3 equiv.) in 0.6 mL benzene-*d*₆ to give a deep-purple solution. Although the ¹⁹F NMR spectrum implied the presence of free B(C₆F₅)₃, the ³¹P NMR resonance at 43.4 ppm became broadened, and the Re-H resonance in the ¹H NMR spectrum disappeared. This all indicated a weak interaction between the Re-H and the boron atom of B(C₆F₅)₃ in solution. Formate formation was not observed. The N₂ atmosphere was then replaced with 1.0 bar of CO₂ using the freeze-pump-thaw cycle. The purple solution turned immediately brown. After 20 min, ³¹P NMR spectroscopy confirmed formation of the intermediate species **2a** in 85 % yield as the only new species. ¹H NMR (300.08 MHz, benzene-*d*₆, ppm): δ 5.72 (dd, ²J_{HP} = 48 Hz, ²J_{HP} = 18 Hz, 1H, ReH), 2.75 (m, 3H, PCH(CH₃)₂), 2.50 (m, 3H, PCH(CH₃)₂), 1.31 (m, 9H, PCH(CH₃)₂), 1.12 (m, 9H, PCH(CH₃)₂), 0.93 (m, 18H, PCH(CH₃)₂). ¹³C{¹H} NMR (75.47 MHz, benzene-*d*₆, ppm): δ 27.1 (d, J_{PC} = 28 Hz, P-CH), 24.6 (d, J_{PC} = 24 Hz, P-CH), 19.2 (s), 19.1 (s), 18.3 (m), 18.0 (s). ³¹P{¹H} NMR (121.47 MHz, benzene-*d*₆, ppm): δ 39.62 (d, ²J_{PP} = 84 Hz, 1P), 33.05 (d, ²J_{PP} = 82 Hz, 1P). ¹⁹F NMR (282.33 MHz, benzene-*d*₆, ppm): δ -134.97 (m, 6F, *ortho*-C₆F₅), -160.07 (t, ¹J_{CF} = 20 Hz, 3F, *para*-C₆F₅), -166.55 (m, 6F, *meta*-C₆F₅). No signals were observed in ¹¹B NMR spectroscopy.

Reaction of **1b with B(C₆F₅)₃ and CO₂ in the NMR tube.** In a 3 mL Young-tap NMR-tube, 17.2 mg **1b** (0.02 mmol) was mixed with 30.1 mg B(C₆F₅)₃ (0.06 mmol, 3 equiv.) in 0.6 mL benzene-*d*₆ to give a deep-purple solution. ¹H, ³¹P and ¹⁹F NMR spectroscopy indicated that reaction had not occurred between **1b** and B(C₆F₅)₃, as the original resonances (for instance Re-H signal at -17.0 ppm in the ¹H NMR) still remained, and no new species formed. The N₂ atmosphere was then replaced with 1.0 bar of CO₂ using a freeze-pump-thaw cycle. Immediately the purple solution turned light brown indicative of formation of the 18e rhenium species **2b**. After 30 min, ³¹P NMR spectroscopy confirmed the quantitative formation of **2b**. Formate was not generated at this stage. ¹H NMR (300.08 MHz, benzene-*d*₆, ppm): δ 6.11 (dd, ²J_{HP} = 48 Hz, ²J_{HP} = 18 Hz, 1H, ReH), 1.03-2.70 (m, 66H, P(C₆H₁₁)₃). ¹³C{¹H} NMR (75.47 MHz, benzene-*d*₆, ppm): δ 37.2 (d,

$J_{\text{PC}} = 26$ Hz, P-CH), 33.9 (d, $J_{\text{PC}} = 23$ Hz, P-CH), 29.6 (s), 29.0 (s), 27.5 (m), 27.0 (s), 26.2 (s). $^{31}\text{P}\{^1\text{H}\}$ NMR (121.47 MHz, benzene- d_6 , ppm): δ 30.00 (d, $^2J_{\text{PP}} = 79$ Hz, 1P), 22.13 ppm (d, $^2J_{\text{PP}} = 79$ Hz, 1P). ^{19}F NMR (282.33 MHz, benzene- d_6 , ppm): δ -134.16 (m, 6F, *ortho*- C_6F_5), -159.99 (t, $^1J_{\text{CF}} = 22$ Hz, 3F, *para*- C_6F_5), -166.47 (m, 6F, *meta*- C_6F_5). ^{11}B NMR signals could not be observed. The transient species is only temporarily stable under CO_2 atmosphere. Exposure of the solution to vacuum leads to back-reaction affording the starting materials **1b**/ $\text{B}(\text{C}_6\text{F}_5)_3$ in over 90 % yield.

Addition of 5 drops of acetonitrile to the benzene solution of the intermediate leads to the quantitative formation of the *trans*-phosphine Re(I) hydride species $[\text{ReHBr}(\text{NO})(\text{PCy}_3)_2(\text{CH}_3\text{CN})]^{15b}$ (^{31}P NMR: δ 16.6 ppm) and $\text{CH}_3\text{CN}\cdot\text{B}(\text{C}_6\text{F}_5)_3$ (^{19}F NMR in benzene- d_6 : δ -130.84 (m, 6F, *ortho*- C_6F_5), -151.68 (t, $^1J_{\text{CF}} = 20$ Hz, 3F, *para*- C_6F_5), -159.48 (m, 6F, *meta*- C_6F_5), or ^{19}F NMR in CD_2Cl_2 : δ -136.22 (m, 6F, *ortho*- C_6F_5), -158.74 (t, $^1J_{\text{CF}} = 20$ Hz, 3F, *para*- C_6F_5), -165.92 (m, 6F, *meta*- C_6F_5)).

[ReBrH₂(NO)(η^1 -OCH=OB(C₆F₅)₃)(P μ Pr₃)₂] (4a): In a 30 mL Young-tap Schlenk vessel placed in glove-box, **3a** (60 mg, 0.025 mmol) was mixed in 2 mL of toluene. The N_2 atmosphere was replaced with 1.0 bar of H_2 using a freeze-pump-thaw cycle. The mixture was kept at 60 °C for 1 h affording a clear light brown solution. After filtration through Celite, the solvent was evaporated *in vacuo*, and the residue was washed with pentane (3 x 2 mL), and dried giving a light brown solid: 61 mg, 99 %. IR (cm^{-1} , ATR): $\nu(\text{NO})$ 1741, $\nu(\text{OC}=\text{O})$ 1595. ^1H NMR (300.08 MHz, toluene- d_8 , ppm): δ 7.71 (s, 1H, OCHO), 3.05 (t, $^2J_{\text{HP}} = 18$ Hz, 2H, η^1 -H₂), 2.20 (m, 6H, PCH(CH₃)₂), 1.15 (m, 18H, PCH(CH₃)₂), 0.82 (m, 18H, PCH(CH₃)₂). $^{13}\text{C}\{^1\text{H}\}$ NMR (75.47 MHz, toluene- d_8 , ppm): δ 173.0 (s, OCHO), 150.3 (s), 147.1 (s), 139.0 (s), 136.2 (s), 23.6 (t, $J_{\text{PC}} = 12$ Hz, P-CH), 18.6 (s, PCH(CH₃)₂). $^{31}\text{P}\{^1\text{H}\}$ NMR (121.47 MHz, toluene- d_8 , ppm): δ 28.5 (s). ^{19}F NMR (282.33 MHz, toluene- d_8 , ppm): δ -134.81 (m, 6F, *ortho*- C_6F_5), -157.74 (t, $^1J_{\text{CF}} = 20$ Hz, 3F, *para*- C_6F_5), -164.98 (m, 6F, *meta*- C_6F_5). Anal. Calcd for $\text{C}_{37}\text{H}_{45}\text{BBrF}_{15}\text{NO}_3\text{P}_2\text{Re}$ (1175.60): C, 37.80; H, 3.86; N, 1.19. Found: C, 38.01; H, 3.74; N, 1.11.

Reaction of 4a with Et₃SiH. In a 3 mL Young-tap NMR-tube, 12 mg of **4a** (0.01 mmol) was mixed with 3.2 μL Et₃SiH (0.02 mmol) in 0.6 mL of toluene- d_8 . After being kept at 100 °C for 5 min, the solution turned from light brown to bright pink. NMR spectroscopy indicated the disappearance of the starting materials (absence of a formate OCHO signal at 7.7 ppm), and the formation of several species.

1) $[\text{HP}\mu\text{Pr}_3][\text{HB}(\text{C}_6\text{F}_5)_3]$ (**5**, 32 %). ^1H NMR (300.08 MHz, toluene- d_8 , ppm): δ 4.40 (dxq, 1H, $^3J_{\text{HH}} = 6$ Hz, $^1J_{\text{HP}} = 453$ Hz, PH). $^{31}\text{P}\{^1\text{H}\}$ NMR (121.47 MHz, toluene- d_8 , ppm): δ 42.6 (s). ^{11}B NMR (96.28 MHz, toluene- d_8 , ppm): δ -19.45 (d, $^1J_{\text{HB}} = 96$ Hz). ^{19}F NMR (282.33 MHz, toluene- d_8 , ppm): δ -134.19 (m, 6F, *ortho*- C_6F_5), -164.48 (m, 3F, *para*- C_6F_5), -167.95 (m, 6F, *meta*- C_6F_5);

2) **1a** (43 %), characterized by its purple color in solution. $^{31}\text{P}\{^1\text{H}\}$ NMR (121.47 MHz, toluene- d_8 , ppm): δ 41.1 (s);

3) $[\text{ReHBr}(\text{NO})(\text{P}\mu\text{Pr}_3)(\eta^4\text{-toluene})]$ (**6**, 25 %). ^1H NMR (300.08 MHz, toluene- d_8 , ppm): δ -7.61 (d, 1H, $^2J_{\text{HP}} = 22$ Hz, ReH). $^{31}\text{P}\{^1\text{H}\}$ NMR (121.47 MHz, toluene- d_8 , ppm): δ 71.5 (s);

4) $(\text{Et}_3\text{SiO})_2\text{CH}_2$ (**7**). ^1H NMR (300.08 MHz, toluene- d_8 , ppm): δ 4.96 (s); 5) $\text{C}=\text{O}\cdot\text{B}(\text{C}_6\text{F}_5)_3$. ^{19}F NMR (282.33 MHz, toluene- d_8 , ppm): δ -134.19 (m, 6F, *ortho*- C_6F_5), -159.81 (m, 3F, *para*- C_6F_5), -164.76 (m, 6F, *meta*- C_6F_5).

Reduction of CO₂ with Et₃SiH catalyzed by "1a/B(C₆F₅)₃". In a 3 mL Young-NMR-tube, 0.25 mmol of Et₃SiH (38 μL) was mixed with 0.6 mL of benzene- d_6 . Then the combination of the catalysts **1a** (1.5 mg, 0.0025 mmol) or **1b** (2.1 mg, 0.0025 mmol) and $\text{B}(\text{C}_6\text{F}_5)_3$ (2.0 mg, 0.0038 mmol) were put on the top of the tube avoiding early mixing with the hydrosilane before charging CO_2 . The N_2 atmosphere was replaced with 1.0 bar of CO_2 using a freeze-pump-thaw cycle. Mixing all the components afforded immediately a light-yellow solution. The mixture was kept at 80 °C and the reaction progress was monitored by

NMR spectroscopy. The color of solution gradually turned darker, and eventually became purple. Alternatively in a 50 mL autoclave vessel, **4a** (6.0 mg, 0.005 mmol) or **3a** (6.0 mg, 0.0025 mmol) were mixed with 0.5 mmol of Et₃SiH (76 μL) in 6 mL of benzene- d_6 . Then 5 bar of CO_2 was charged and the reaction was kept at 80 °C for 13 h. The TON and TOF values were determined based on the consumption of the hydrosilane. The composition of the products was determined by ^1H NMR and GC-MS. Characteristic NMR resonances:

$(\text{Et}_3\text{SiO})_2\text{CH}_2$ (**7**). ^1H NMR (300.08 MHz, benzene- d_6 , ppm): δ 5.07 (s), 1.05 (t, $J = 9$ Hz, CH_3), 0.67 (q, $J = 6$ Hz, SiCH_2). ^{29}Si NMR (90 MHz, benzene- d_6 , ppm): δ 18.90 (s);

$\text{Et}_3\text{SiOCH}_3$ (**9**). ^1H NMR (300.08 MHz, benzene- d_6 , ppm): δ 3.32 (s).

Hydrogenation of CO₂ catalyzed by "1/B(C₆F₅)₃" in the presence of bases. In a 50 mL autoclave vessel, 0.005 mmol of [Re] (**1a**, 3.1 mg; **1b**, 4.3 mg; **3a**, 5.9 mg; **4a**, 5.9 mg) and 0.01 mmol of $\text{B}(\text{C}_6\text{F}_5)_3$ (5.4 mg) were mixed with 1.0 mmol of base (TMP, 170 μL ; HNiPr_2 , 140 μL ; NEt_3 , 150 μL ; HNCy_2 , 200 μL ; PtBu_3 , 250 μL ; $\text{HN}(\text{SiMe}_3)_2$, 208 μL ; 2,4,6-tri-*tert*-butylpyridine, 250 mg) in 1 mL of solvent (THF or chlorobenzene). Afterwards the autoclave was charged with 20 bar of CO_2 and 40 bar of H_2 . The mixture was kept at 80 °C for overnight. After cooling to room temperature, 10 μL of DMF (0.13 mmol) was added to the resultant solution as an internal standard. An aliquot of the mixture (50 μL) was mixed in 0.5 mL of D_2O or CDCl_3 and examined by ^1H NMR spectroscopy. The yield was calculated from the integration of the signal of the formate proton (δ 8.5, s) and that of DMF (δ 7.9, s). After removing the solvent, the residue was washed with Et₂O (3 x 2 mL), dried giving off-white solids, which were identified to be the formate salts.

$[\text{H}\cdot\text{TMP}]^+[\text{O}\cdot\text{CH}=\text{O}]^-$ (**11**). Isolated: 37 mg. Yield: 20 %. ^1H NMR (300.08 MHz, D_2O , ppm): δ 8.44 (s, 1 H, CHO), 1.75 (m, 2 H), 1.65 (m, 4 H), 1.39 (s, 12 H). ^1H NMR (300.08 MHz, CDCl_3 , ppm): δ 8.70 (s, 1 H, CHO), 3.75 (s, 2H, NH), 2.17 (m, 2 H), 1.69 (m, 4 H), 1.45 (s, 12 H). ^{13}C NMR (75.47 MHz, D_2O , ppm): δ 171.4 (s), 57.2 (s), 34.9 (s), 27.1 (s), 16.1 (s). IR (cm^{-1} , ATR): 2947 (s), 2644 (s), 2596 (br), 2502 (br), 1587 (s, C=O). MS (ESI): m/z : 142.2 ($[\text{H}\cdot\text{TMP}]^+$). Anal. Calcd for $\text{C}_{10}\text{H}_{21}\text{NO}_2$ (187.16): C, 64.13; H, 11.30; N, 7.48. Found: C, 64.39; H, 11.25; N, 7.30.

$[\text{H}_2\text{N}\mu\text{Pr}_2]^+[\text{O}\cdot\text{CH}=\text{O}]^-$ (**16**). Isolated: 18 mg. Yield: 12 %. ^1H NMR (300.08 MHz, CDCl_3 , ppm): δ 8.58 (s, 1 H, CHO), 3.75 (br, 2H, NH), 3.42 (m, $^3J_{\text{HH}} = 6$ Hz, 2H), 1.44 (d, $^3J_{\text{HH}} = 6$ Hz, 12H). ^{13}C NMR (75.47 MHz, CDCl_3 , ppm): δ 168.1 (s), 47.3 (s), 19.2 (s). IR (cm^{-1} , ATR): 2979 (s), 2864 (br), 2676 (s), 2492 (br), 1626 (s, C=O), 1555 (s). MS (ESI): m/z : 102.4 ($[\text{H}_2\text{N}\mu\text{Pr}_2]^+$).

$[\text{H}_2\text{NCy}_2]^+[\text{O}\cdot\text{CH}=\text{O}]^-$ (**17**). Isolated: 30 mg. Yield: 13 %. ^1H NMR (300.08 MHz, D_2O , ppm): δ 8.31 (s, 1 H, CHO), 3.06 (m, 2H, N-CH), 1.16-1.91 (m, 20 H). ^1H NMR (300.08 MHz, CDCl_3 , ppm): δ 8.60 (s, 1 H, CHO), 3.74 (br, 2H, NH), 3.00 (m, 2H, N-CH), 1.23-2.09 (m, 20H). ^{13}C NMR (75.47 MHz, D_2O , ppm): δ 171.4 (s), 53.6 (s), 29.9 (s), 25.2 (s), 24.5 (s). ^{13}C NMR (75.47 MHz, CDCl_3 , ppm): δ 168.1 (s), 52.8 (s), 29.2 (s), 25.1 (s), 24.8 (s). IR (cm^{-1} , ATR): 2936 (s), 2857(s), 2756 (s), 2671 (s), 1630 (s, C=O), 1548 (s). MS (ESI): m/z : 182.1 ($[\text{H}_2\text{NCy}_2]^+$). Anal. Calcd for $\text{C}_{13}\text{H}_{25}\text{NO}_2$ (227.19): C, 68.68; H, 11.08; N, 6.16. Found: C, 68.72; H, 10.98; N, 6.05.

Computational Methods. All calculations were performed with the *Gaussian03* program package²⁷ using the functional B3LYP²⁸ in combination with the Stuttgart/Dresden effective core potentials (SDD) basis set²⁹ for Re and the standard 6-31+G(d)³⁰ for the remaining atoms. Sum of electronic and zero-point energies are taken as relative energies.

Crystallographic studies of compounds 3a and 11. Single-crystal X-ray diffraction data were collected at 183(2) K on a *Xcalibur* diffractometer (Agilent Technologies, Ruby CCD detector) using a single wavelength Enhance X-ray source with MoK α radiation ($\lambda = 0.71073$ Å) for **3a** and on a *Supernova* area-detector diffractometer using a high intensity copper (Cu) X-ray micro-source ($\lambda = 1.54184$ Å) for **11**.³¹

The selected suitable single crystals were mounted using polybutene oil on the top of a glass fiber fixed on a goniometer head and immediately transferred to the diffractometer. Pre-experiment, data collection, data reduction and analytical absorption corrections³² were performed with the program suite *CrysAlis^{Pro}*.³¹ The crystal structures were solved with *SHELXS97*³³ using direct methods. The structure refinements were performed by full-matrix least-squares on F² with *SHELXL97*.³³ All programs used during the crystal structure determination process are included in the *WINGX* software.³⁴ *PLATON*³⁵ was used to check the result of the X-ray analyses. For more details about the refinements, see the *_exptl_special_details* and *iucr_refine_instructions_details* sections in the Crystallographic Information files (Supporting Information). CCDC-927599 (for **3a**) and CCDC-927600 (for **11**) contain the supplementary crystallographic data for this paper. These data can be obtained free of charge from The Cambridge Crystallographic Data Centre via www.ccdc.cam.ac.uk/data_request/cif.

ASSOCIATED CONTENT

Supporting Information. Crystallographic details and the CIF file of **3a** and **11**, computational details, and NMR spectra for CO₂ activation and reduction courses. This material is available free of charge via the Internet at <http://pubs.acs.org>.

AUTHOR INFORMATION

Corresponding Author

hberke@aci.uzh.ch

Notes

The authors declare no competing financial interest.

ACKNOWLEDGMENT

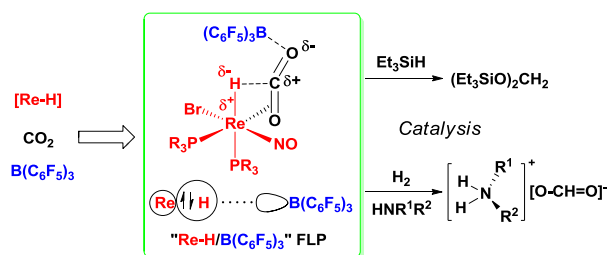
Financial support from the Swiss National Science Foundation, Lanxess AG, Leverkusen, Germany, the Funds of the University of Zurich, the DFG and SNF within the project 'Forschergruppe 1175 - Unconventional Approaches to the Activation of Dihydrogen' are gratefully acknowledged.

REFERENCES

- (1) (a) Angamuthu, R.; Byers, P.; Lutz, M.; Spek, A. L.; Bouwman, E. *Science* **2010**, *327*, 313. (b) Das Neves Gomes, C.; Jacquet, O.; Villers, C.; Thuery, P.; Ephritikhine, M.; Cantat, T. *Angew. Chem. Int. Ed.* **2012**, *51*, 187.; (c) Lewis, N. S.; Nocera, D. G. *Proc. Natl. Acad. Sci. U.S.A.* **2006**, *103*, 15729.; (d) Olah, G. A. *Angew. Chem. Int. Ed.*, **2005**, *44*, 2636.; (e) Olah, G. A.; Prakash, G. K. S.; Goepfert, A. *J. Org. Chem.* **2009**, *74*, 487.
- (2) For "M/H₂": (a) Gassner, F.; Leitner, W. *J. Chem. Soc., Chem. Commun.* **1993**, 1465.; (b) Jessop, P. G.; Ikariya, T.; Noyori, R. *Nature*, **1994**, *368*, 231.; (d) Munshi, P.; Main, A. D.; Linehan, J. C.; Tai, C. C.; Jessop, P. G. *J. Am. Chem. Soc.* **2002**, *124*, 7963.; (e) Himeda, Y.; Onozawa-Komatsuzaki, N.; Sugihara, H.; Kasuga, K. *Organometallics* **2007**, *26*, 702.; (f) Tanaka, R.; Yamashita, M.; Nozaki, K. *J. Am. Chem. Soc.* **2009**, *131*, 14168.; (g) Federsel, C.; Boddien, A.; Jackstell, R.; Jennerjahn, R.; Dyson, P. J.; Scopelliti, R.; Laurenczy, G.; Beller, M. *Angew. Chem. Int. Ed.* **2010**, *49*, 9777.; (h) Cokoja, M.; Bruckmeier, C.; Rieger, B.; Herrmann, W. A.; Kühn, F. E. *Angew. Chem. Int. Ed.* **2011**, *50*, 8510.; (i) Langer, R.; Diskin-Posner, Y.; Leitner, G.; Shimon, L. J. W.; Ben-David, Y.; Milstein, D. *Angew. Chem. Int. Ed.* **2011**, *50*, 9948.; (j) Huff, C. A.; Sanford, M. S. *J. Am. Chem. Soc.* **2011**, *133*, 18122.; (k) Wesselbaum, S.; vom Stein T.; Klankermayer, J.; Leitner, W. *Angew. Chem. Int. Ed.* **2012**, *51*, 7499.
- (3) For "M/Silane": (a) Eisenschmid, T. C.; Eisenberg, R. *Organometallics* **1989**, *8*, 1822.; (b) Matsuo, T.; Kawaguchi, H. *J. Am. Chem. Soc.* **2006**, *128*, 12362.; (c) Park, S.; Bezier, D.; Brookhart, M. *J. Am. Chem. Soc.* **2012**, *134*, 11404.; (d) Riduan, S. N.; Zhang, Y. *Dalton. Trans.* **2010**, *39*,

- 3347.; (e) Deglmann, P.; Ember, E.; Hofmann, P.; Pitter, S.; Walter, O. *Chem. Eur. J.* **2007**, *13*, 2864.; (f) Jessop, P. G.; Ikariya, T.; Noyori, R. *Chem. Rev.* **1999**, *99*, 475.
- (4) For "M/Borane": (a) Laitar, D. S.; Müller, P.; Sadighi, J. P. *J. Am. Chem. Soc.* **2005**, *127*, 17196.; (b) Chakraborty, S.; Zhang, J.; Krause, J. A.; Guan, H. *J. Am. Chem. Soc.* **2010**, *132*, 8872.; (c) Huang, F.; Zhang, C.; Jiang, J.; Wang, Z.-X.; Guan, H. *Inorg. Chem.* **2011**, *50*, 3816.; (d) Bontemp, S.; Vendier, L.; Sabo-Etienne, S. *Angew. Chem. Int. Ed.* **2012**, *51*, 1671.
- (5) For "NHCs": (a) Lavigne, F.; Maerten, E.; Alcaraz, G.; Branchadell, V.; Saffon-Merceron, N.; Baccaredo, A. *Angew. Chem. Int. Ed.* **2012**, *51*, 2489.; (b) Kayaki, Y.; Yamamoto, M.; Ikariya, T. *Angew. Chem. Int. Ed.* **2009**, *48*, 4194.; (c) Riduan, S. N.; Zhang, Y.; Ying, J. Y. *Angew. Chem. Int. Ed.* **2009**, *48*, 3322.; (d) Gu, L.; Zhang, Y. *J. Am. Chem. Soc.* **2010**, *132*, 914.; (e) Jacquet, O.; Des Neves Gomes, C.; Ephritikhine, M.; Cantat, T. *J. Am. Chem. Soc.* **2012**, *134*, 2934.
- (6) For "Silylium": Schäfer, A.; Saak, W.; Haase, D.; Müller, T. *Angew. Chem. Int. Ed.* **2012**, *51*, 2981.
- (7) For "[Et₃Al]⁺": Khandelwal, M.; Wehmschulte, R. *J. Angew. Chem. Int. Ed.* **2012**, *51*, 1.
- (8) For reviews of FLPs: (a) Stephan, D. W.; Erker, G. *Angew. Chem. Int. Ed.* **2010**, *49*, 46.; (b) Stephan, D. W. *Dalton. Trans.* **2009**, 3129.
- (9) Special issue on "Frustrated Lewis Pairs" in *Dalton. Trans.* **2012**, *41*, 8999-9045.
- (10) For "B/P": (a) Mömning, C. M.; Otten, E.; Kehr, G.; Fröhlich, R.; Grimme, S.; Stephan, D. W.; Erker, G. *Angew. Chem. Int. Ed.* **2009**, *48*, 6643.; (b) Hounjet, L. J.; Caputo, C. B.; Stephan, D. W. *Angew. Chem. Int. Ed.* **2012**, *51*, 4714.; (c) Peuser, I.; Neu, R. C.; Zhao, X.; Ulrich, M.; Schirmer, B.; Tannert, J. A.; Kehr, G.; Fröhlich, R.; Grimme, S.; Erker, G.; Stephan, D. W. *Chem. Eur. J.* **2011**, *17*, 9640.; (d) Harhausen, M.; Fröhlich, R.; Kehr, G.; Erker, G. *Organometallics* **2012**, *31*, 2801.
- (11) For "B/N": (a) Ashley, A. E.; Thompson, A. L.; O'Hare, D. *Angew. Chem. Int. Ed.* **2009**, *48*, 9839.; (b) Berkefeld, A.; Piers, W. E.; Parvez, M. J. *J. Am. Chem. Soc.* **2010**, *132*, 10660.; (c) Khalimon, A. Y.; Piers, W. E.; Blackwell, J. M.; Michalak, D. J.; Parvez, M. *J. Am. Chem. Soc.* **2012**, *134*, 9601.; (d) Voss, T.; Mahdi, T.; Otten, E.; Fröhlich, R.; Kehr, G.; Stephan, D. W.; Erker, G. *Organometallics* **2012**, *31*, 2367.
- (12) For "Al/P": (a) Menard, G.; Stephan, D. W. *J. Am. Chem. Soc.* **2010**, *132*, 1796.; (b) Menard, G.; Stephan, D. W. *Angew. Chem. Int. Ed.* **2011**, *50*, 8396.; (c) Appelt, C.; Westenberg, H.; Bertini, F.; Ehlers, A. W.; Slootweg, J. C.; Lammertsma, K.; Uhl, W. *Angew. Chem. Int. Ed.* **2011**, *50*, 3925.; (d) Boudreau, J.; Courtemanche, M. A.; Fontaine, F. G. *Chem. Commun.*, **2011**, *47*, 11131.; (e) Menard, G.; Stephan, D. W. *Angew. Chem. Int. Ed.* **2012**, *51*, 8272.
- (13) For "M-H/CO₂": (a) Pu, L. S.; Yamamoto, A.; Ikeda, S. *J. Am. Chem. Soc.* **1968**, *90*, 3896.; (b) Darensbourg, D. J. *Inorg. Chem.* **2010**, *49*, 10765.; (c) Musashi, Y.; Sakaki, S. *J. Am. Chem. Soc.* **2000**, *122*, 3867.; (d) Yin, X.; Moss, J. R. *Coord. Chem. Rev.* **1999**, *181*, 27.; (e) Gibson, D. H. *Coord. Chem. Rev.* **1999**, *185-186*, 335.; (f) Yin, C.; Xu, Z.; Yang, S. Y.; Ng, S. M.; Wong, K. Y.; Lin, Z.; Lau, C. P. *Organometallics* **2001**, *20*, 1216.
- (14) For transition metal involved FLPs: (a) Chapman, A. M.; Haddow, M. F.; Wass, D. F. *J. Am. Chem. Soc.* **2011**, *133*, 18463.; (b) Sgro, M. J.; Stephan, D. W. *Angew. Chem. Int. Ed.* **2012**, *51*, 11343.
- (15) (a) Jiang, Y.; Blacque, O.; Fox, T.; Frech, C. M.; Berke, H. *Chem. Eur. J.* **2009**, *15*, 2121.; (b) Jiang, Y.; Blacque, O.; Fox, T.; Frech, C. M.; Berke, H. *Organometallics* **2009**, *28*, 5493.; (c) Jiang, Y.; Blacque, O.; Fox, T.; Frech, C. M.; Berke, H. *Organometallics* **2009**, *28*, 4670.; (d) Jiang, Y.; Blacque, O.; Fox, T.; Frech, C. M.; Berke, H. *Chem. Eur. J.* **2010**, *16*, 2240.; (e) Jiang, Y.; Hess, J.; Fox, T.; Berke, H. *J. Am. Chem. Soc.* **2010**, *132*, 18233.
- (16) Saverio, A. D.; Focante, F.; Camurati, I.; Resconi, L.; Beringhelli, T.; D'Alfonso, G.; Donghi, D.; Maggioni, D.; Mercandelli, P.; Sironi, A. *Inorg. Chem.* **2005**, *44*, 5030.
- (17) For Os: (a) Kuhlman, R.; Streib, W. E.; Huffman, J. C.; Caulton, K. G. *J. Am. Chem. Soc.* **1996**, *118*, 6934.; (b) Esteruelas, M. A.; Lopez, A. M.; Onate, E.; Royo, E. *Organometallics* **2005**, *24*, 5780.; For Rh: (c) Cheliat-sidou, P.; White, D. F. S.; de Bruin, B.; Reek, J. N. H.; Cole-Hamilton, D. J. *Organometallics* **2007**, *26*, 3265.

- (18) (a) Höck, J.; Jacobsen, H.; Schmalle, H. W.; Artus, G. R. J.; Fox, T.; Amor, J. I.; B ath, F.; Berke, H. *Organometallics* **2001**, *20*, 1533; (b) Zhao, Y.; Schmalle, H. W.; Fox, T.; Blacque, O.; Berke, H. *Dalton. Trans.*, **2006**, 73.
- (19) Gusev, D.; Llamazares, A.; Artus, G.; Jacobsen, H.; Berke, H. *Organometallics* **1999**, *18*, 75.
- (20) Jiang, Y.; Blacque, O.; Fox, T.; Berke, H. *J. Am. Chem. Soc.* **2013**, *135*, 4088.
- (21) Landwehr, A.; Dudle, B.; Fox, T.; Blacque, O.; Berke, H. *Chem. Eur. J.* **2012**, *18*, 5701.
- (22) (a) Noyori, R.; Ohkuma, T. *Angew. Chem., Int. Ed.* **2001**, *40*, 40; (b) Noyori, R.; Yamakawa, M.; Hashiguchi, S. *J. Org. Chem.* **2001**, *66*, 7931; (c) Morris, R. H. *Chem. Soc. Rev.* **2009**, *38*, 2282; (d) Morris, R. H. *Coord. Chem. Rev.* **2008**, *252*, 2381; (e) Clapham, S. E.; Hadzovic, A.; Morris, R. H. *Coord. Chem. Rev.* **2004**, *248*, 2201; (f) Gruetzmacher, H. *Angew. Chem., Int. Ed.* **2008**, *47*, 1814; (g) Ingleson, M. J.; Brayshaw, S. K.; Mahon, M. F.; Ruggiero, G. D.; Weller, A. S. *Inorg. Chem.* **2005**, *44*, 3162; (h) Kubas, G. J. *Adv. Inorg. Chem.*, **2004**, *56*, 127; (i) Yi, C. S.; Lee, D. W.; He, Z.; Rheingold, A. L.; Lam, K.-C.; Concolino, T. E. *Organometallics* **2000**, *19*, 2909; (j) Heinekey, D. M.; Lledos, A.; Lluch, J. M.; *Chem. Soc. Rev.* **2004**, *33*, 175.
- (23) Ilyin, P. V.; Pankova, A. S.; Kuznetsov, M. A. *Synthesis*, **2012**, *44*, 1353.
- (24) Jeffrey, G. A. *An introduction to hydrogen bonding*, **1997**, Oxford University Press.
- (25) (a) Heinekey, D. M.; Millar, J. M.; Koetzle, T. F.; Payne, N. G.; Zilm, K. W. *J. Am. Chem. Soc.* **1990**, *112*, 909; (b) Dudle, B.; Rajesh, K.; Blacque, O.; Berke, H. *J. Am. Chem. Soc.* **2011**, *133*, 8168.
- (26) (a) Maseras, F.; Lledos, A.; Clot, E.; Eisenstein, O. *Chem. Rev.* **2000**, *100*, 601; (b) Kubas, G. J. *Chem. Rev.* **2007**, *107*, 4152.
- (27) Frisch, M. J.; Trucks, G. W.; Schlegel, H. B.; Scuseria, G. E.; Robb, M. A.; Cheeseman, J. R.; Montgomery, J. A., Jr.; T. V.; Kudin, K. N.; Burant, J. C.; Millam, J. M.; Iyengar, S. S.; Tomasi, J.; Barone, V.; Mennucci, B.; Cossi, M.; Scalmani, G.; Rega, N.; Petersson, G. A.; Nakatsuji, H.; Hada, M.; Ehara, M.; Toyota, K.; Fukuda, R.; Hasegawa, J.; Ishida, M.; Nakajima, T.; Honda, Y.; Kitao, O.; Nakai, H.; Klene, M.; Li, X.; Knox, J. E.; Hratchian, H. P.; Cross, J. B.; Adamo, C.; Jaramillo, J.; Gomperts, R.; Stratmann, R. E.; Yazyev, O.; Austin, A. J.; Cammi, R.; Pomelli, C.; Ochterski, J. W.; Ayala, P. Y.; Morokuma, K.; Voth, G. A.; Salvador, P.; Dannenberg, J. J.; Zakrzewski, G.; Dapprich, S.; Daniels, A. D.; Strain, M. C.; Farkas, O.; Malick, D. K.; Rabuck, A. D.; Raghavachari, K.; Foresman, J. B.; Ortiz, J. V.; Cui, Q.; Baboul, A. G.; Clifford, S.; Cioslowski, J.; Stefanov, B. B.; Liu, G.; Liashenko, A.; Piskorz, P.; Komaromi, I.; Martin, R. L.; Fox, D. J.; Keith, T.; Al-Laham, M. A.; Peng, C. Y.; Nanayakkara, A.; Challacombe, M.; Gill, P. M. W.; Johnson, B.; Chen, W.; Wong, M. W.; Gonzalez, C.; Pople, J. A. Gaussian 03, revision D.01, Gaussian, Inc., Wallingford, CT, **2003**.
- (28) (a) Becke, A. D. *J. Chem. Phys.*, **1993**, *98*, 5648; (b) Lee, C.; Yang, W.; and Parr, R. G. *Phys. Rev. B*, **1988**, *37*, 785; (c) Miehlich, B.; Savin, A.; Stoll, H.; Preuss, H. *Chem. Phys. Lett.*, **1989**, *157*, 200.
- (29) T. H. Dunning Jr, P. J. Hay, *Modern Theoretical Chemistry*, Plenum, New York, **1976**.
- (30) Ditchfield, R.; Hehre, W. J.; Pople, J. A. *J. Chem. Phys.* **1971**, *54*, 724.
- (31) Agilent Technologies (formerly Oxford Diffraction), Yarnton, England **2011**.
- (32) Clark, R. C.; Reid, J. S. *Acta Crystallogr A*. **1995**, *51*, 887.
- (33) Sheldrick, G. *Acta Crystallogr A*. **2008**, *64*, 112.
- (34) Farrugia, L. *J Appl Crystallogr* **1999**, *32*, 837.
- (35) Spek, A. L. *J Appl Crystallogr* **2003**, *36*, 7.



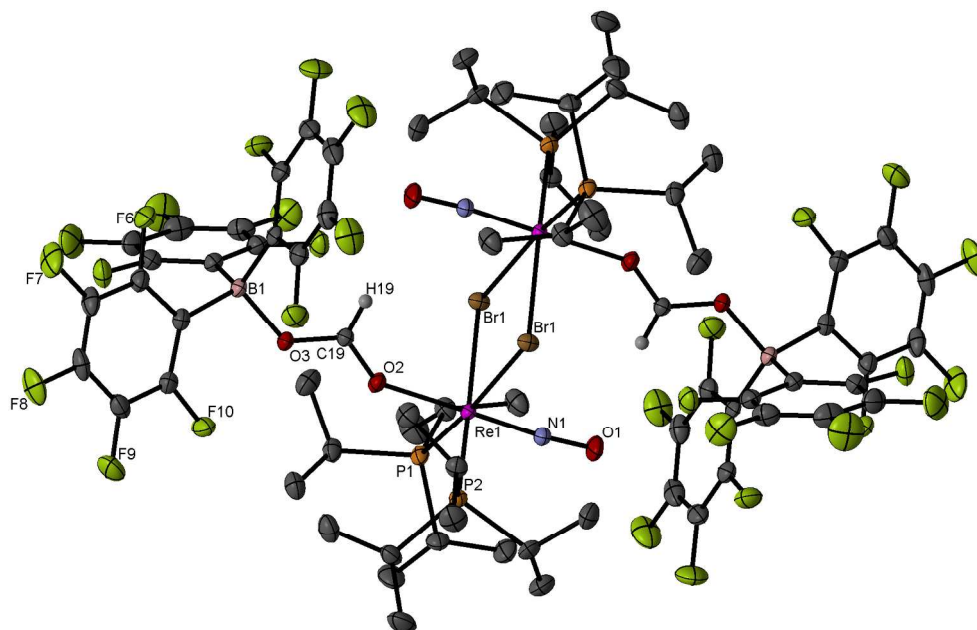
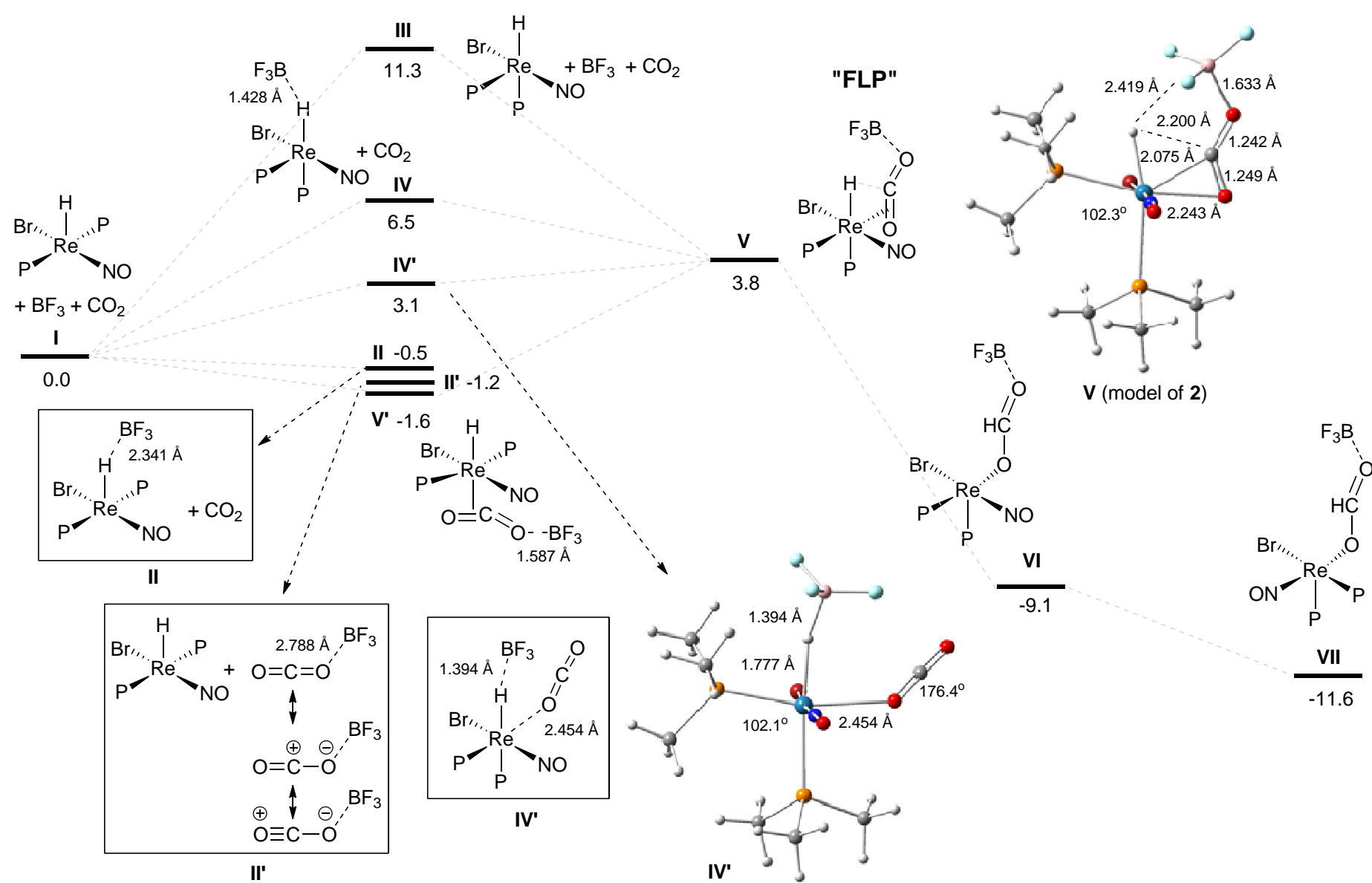


Figure 1. Molecular structure of 3a with 30 % probability displacement ellipsoids. All hydrogen atoms were omitted for clarity except for the formate moieties. Selected bond lengths (Å) and angles (deg): N(1)-O(1), 1.192(2); O(2)-Re(1), 2.1164(15); Re(1)-P(1), 2.4675(7); Re(1)-P(2), 2.4713(6); O(3)-B(1), 1.553(3); C(19)-O(2), 1.246(2); C(19)-O(3), 1.268(3); O(1)-N(1)-Re(1), 174.63(18); C(19)-O(2)-Re(1), 144.74(16); N(1)-Re(1)-O(2), 178.66(8); P(1)-Re(1)-P(2), 103.78(2); C(19)-O(3)-B(1), 126.52(18).
559x353mm (96 x 96 DPI)



1
2
3
4
5
6
7
8
9
10
11
12
13
14
15
16
17
18
19
20
21
22
23
24
25
26
27
28
29
30
31
32
33
34
35
36
37
38
39
40
41
42
43
44
45
46
47
48
49
50
51
52
53
54
55
56
57
58
59
60

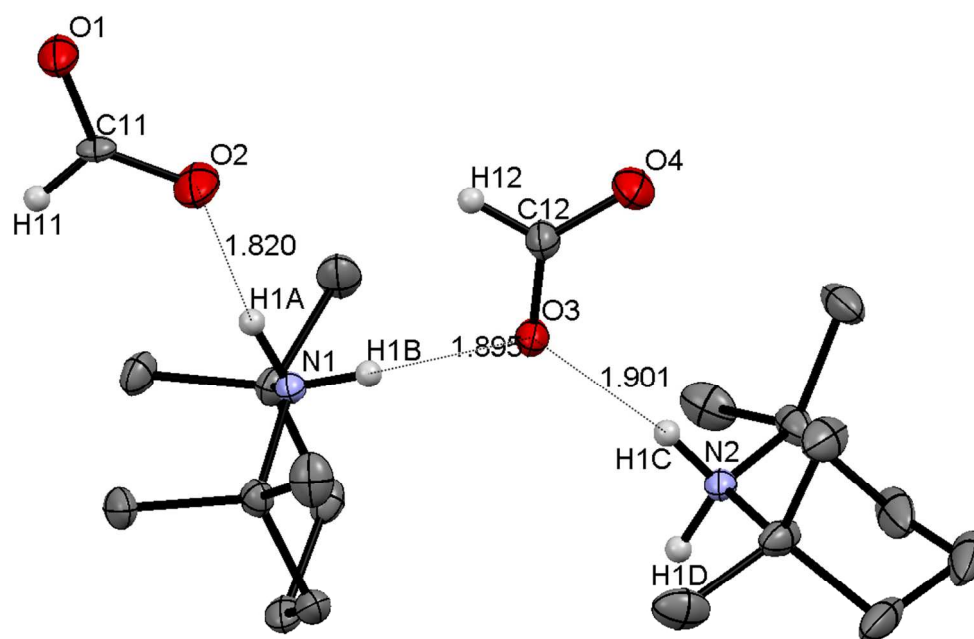
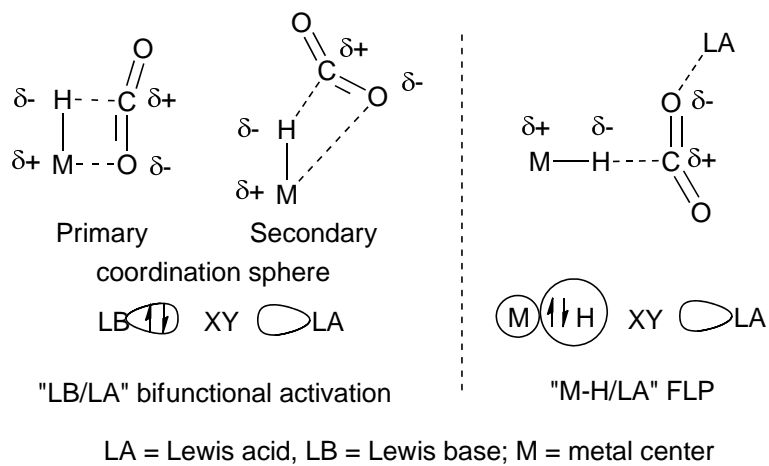
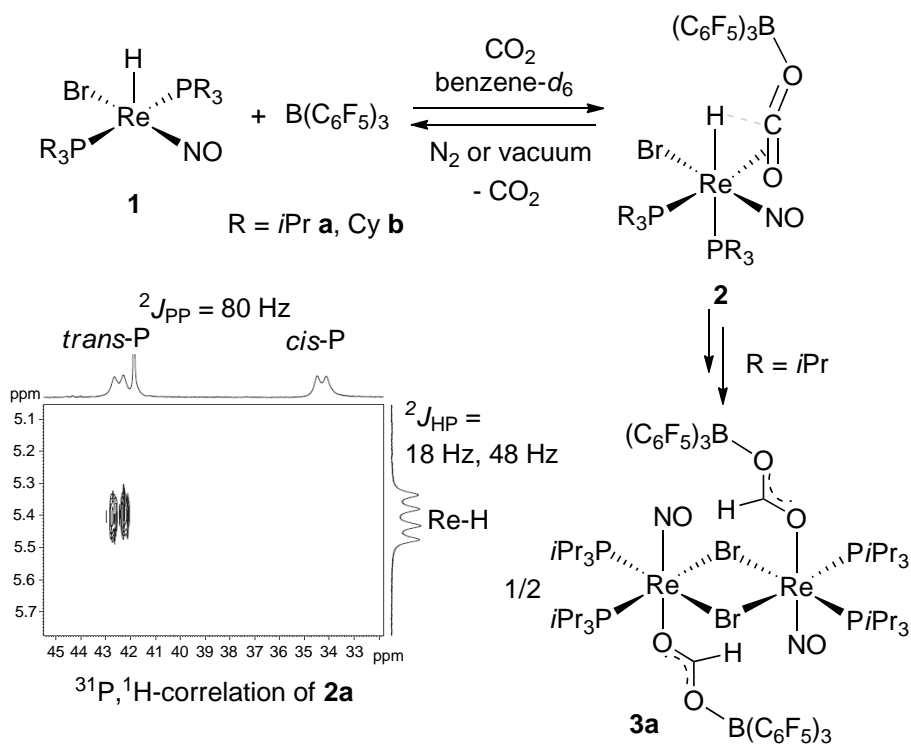
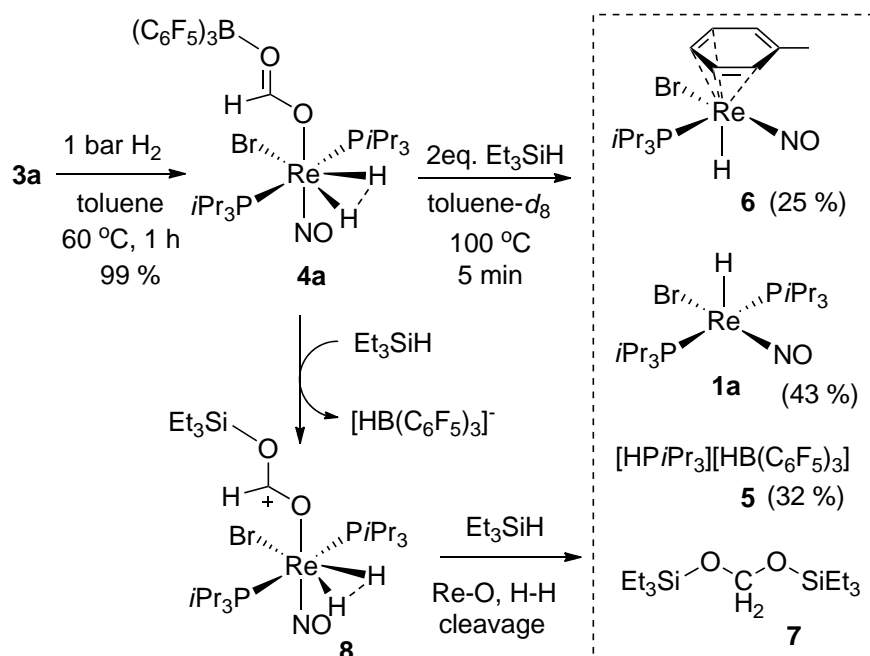
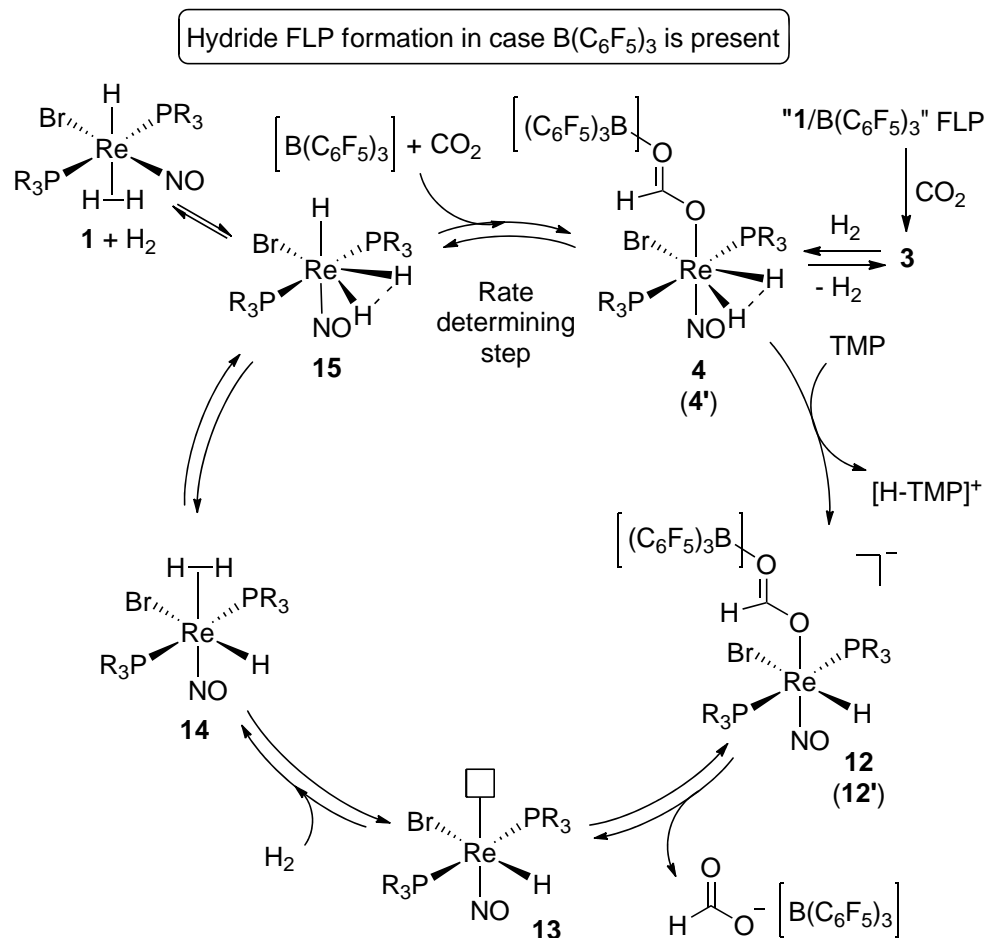


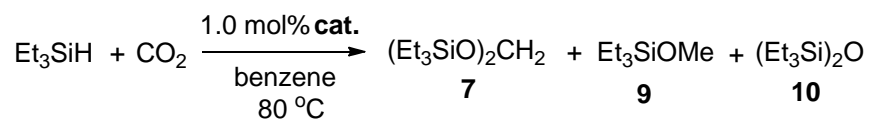
Figure 3. Molecular structure of 11 with 30 % probability displacement ellipsoids. All hydrogen atoms were omitted for clarity except for the formate and NH₂ moieties.
295x201mm (96 x 96 DPI)





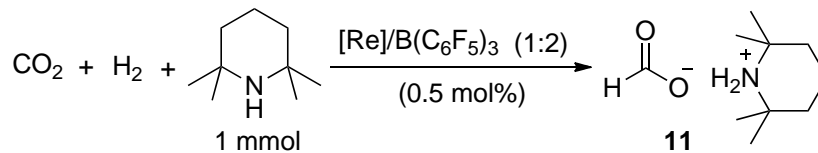






Entry	cat.	P_{CO_2} (bar)	t (h)	Yield (%) ^a 7 / 9 / 10	TON	TOF (h ⁻¹)
1	1a /B(C ₆ F ₅) ₃ ^b	1	4	35 / 0 / 0	35	8.8
2	1b /B(C ₆ F ₅) ₃ ^b	1	4	18 / 0 / 0	18	4.5
3	3a	5	15	87 / 1 / 1	89	5.9
4	4a	5	13	89 / 3 / 3	95	7.3

^a Determined by GC-MS. ^b In a ratio of 1:1.5



15
16
17
18
19
20
21
22
23
24
25
26
27
28
29
30
31
32
33
34
35

Entry	[Re]	solvent	T(°C)	$P_{\text{H}_2/\text{CO}_2}$ (bar)	t (h)	Conv. (%) ^a	TON	TOF (h ⁻¹)
1	1a	C ₆ H ₅ Cl	80	40/20	15	8	15	1.0
2	1a	THF	80	40/20	15	52 ^b	104	6.9
3	1a	THF	80	40/20	2	8	16	7.5
4	--	THF	80	40/20	24	0	0	0
5	1a	THF	23	40/20	18	0	0	0
6	1a	THF	120	40/20	18	3	6	0.3
7	1a	THF	80	20/10	15	4	8	0.4
8	1b	THF	80	40/20	16	28	55	3.4
9 ^c	3a	THF	80	40/20	15	36	72	4.8
10 ^c	4a	THF	80	40/20	15	46	92	6.1
11 ^c	1a	THF	80	40/20	15	39	78	5.2
12 ^c	1a	MeOH	80	40/20	15	25	50	3.3

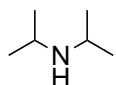
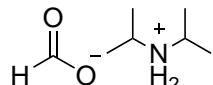
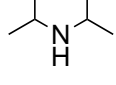
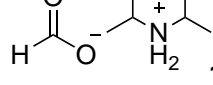
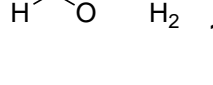
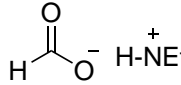
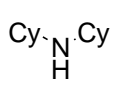
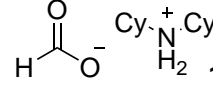
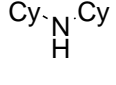
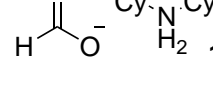
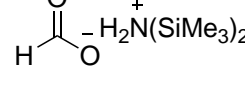
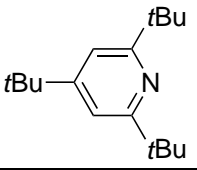
36
37
38
39
40
41
42
43
44
45
46
47
48
49
50
51
52
53
54
55
56
57
58
59
60

^a Determined by referring to the internal standard DMF in ¹H NMR spectra. ^b in 20 % isolated yield. ^c in the absence of B(C₆F₅)₃

1
2
3
4
5
6
7
8
9
10
11
12
13
14
15
16
17
18
19
20
21
22
23
24
25
26
27
28
29
30
31
32
33
34
35
36
37
38
39
40
41
42
43
44
45
46
47
48
49
50
51
52
53
54
55
56
57
58
59
60

$$\text{CO}_2 + \text{H}_2 + \text{base} \xrightarrow[\text{THF, 80 } ^\circ\text{C}]{\begin{matrix} 0.5 \text{ mol\% [Re]} \\ 1.0 \text{ mol\% B(C}_6\text{F}_5)_3 \end{matrix}} \text{H}-\text{C}(=\text{O})-\text{O}^- [\text{H-base}]^+$$

20 bar 40 bar 1 mmol

Entry	[Re]	base	product	t(h)	Conv. (%) ^a	TON	TOF (h ⁻¹)
1	1a			34	87 ^b	174	5.1
2	1b			36	67	134	3.7
3 ^c	1a			15	27	54	3.6
4	1a			22	3	7	0.3
5	1b	NEt ₃		28	5	10	0.4
6 ^c	1a			18	3	6	0.3
7	1a	PtBu ₃	---	16	<1	--	--
8	1a			30	61 ^d	122	4.1
9 ^c	1a			20	34	68	3.4
10	1a	HN(SiMe ₃) ₂		16	2	4	0.2
11 ^e	1a		---	6	--	--	--

^a Determined by referring to the internal standard DMF in ¹H NMR spectra. ^b in 12 % isolated yield. ^c in the absence of B(C₆F₅)₃. ^d In 13 % isolated yield. ^e with 10 mol% of **1a**/B(C₆F₅)₃ (1:2)

